ORIGINAL ARTICLE

Mutations in apoptosis-inducing factor cause X-linked recessive auditory neuropathy spectrum disorder

Liang Zong,[1] Jing Guan,[1] Megan Ealy,[2,3] Qiujing Zhang,[1] Dayong Wang,[1] Hongyang Wang,[1] Yali Zhao,[1,4] Zhirong Shen,[5] Colleen A Campbell,[2] Fengchao Wang,[5] Ju Yang,[1] Wei Sun,[6] Lan Lan,[1] Dalian Ding,[6] Linyi Xie,[1] Yue Qi,[1] Xin Lou,[7] Xusheng Huang,[8] Qiang Shi,[8] Suhua Chang,[9] Wenping Xiong,[1] Zifang Yin,[1] Ning Yu,[1] Hui Zhao,[1] Jun Wang,[10] Jing Wang,[9] Richard J Salvi,[6] Christine Petit,[11] Richard J H Smith,[2] Qiuju Wang[1]

▶ Additional material is published online only. To view please visit the journal online (http://dx.doi.org/10.1136/jmedgenet-2014-102961).

For numbered affiliations see end of article.

Correspondence to
Professor Qiuju Wang, Department of Otolaryngology-Head and Neck Surgery, Institute of Otolaryngology, PLA General Hospital, 28 Fuxing Road, Beijing 100853, China; wqcr301@sina.com

Professor Richard JH Smith, Department of Otolaryngology-Head and Neck Surgery, University of Iowa, Iowa City, IA 52242, USA; richard-smith@uiowa.edu

LZ, JG, ME contributed equally to this work.

Received 17 December 2014
Revised 6 April 2015
Accepted 21 April 2015
Published Online First 18 May 2015

To cite: Zong L, Guan J, Ealy M, *et al*. *J Med Genet* 2015;**52**:523–531.

ABSTRACT

Background Auditory neuropathy spectrum disorder (ANSD) is a form of hearing loss in which auditory signal transmission from the inner ear to the auditory nerve and brain stem is distorted, giving rise to speech perception difficulties beyond that expected for the observed degree of hearing loss. For many cases of ANSD, the underlying molecular pathology and the site of lesion remain unclear. The X-linked form of the condition, AUNX1, has been mapped to Xq23-q27.3, although the causative gene has yet to be identified.

Methods We performed whole-exome sequencing on DNA samples from the AUNX1 family and another small phenotypically similar but unrelated ANSD family.

Results We identified two missense mutations in *AIFM1* in these families: c.1352G>A (p.R451Q) in the AUNX1 family and c.1030C>T (p.L344F) in the second ANSD family. Mutation screening in a large cohort of 3 additional unrelated families and 93 sporadic cases with ANSD identified 9 more missense mutations in *AIFM1*. Bioinformatics analysis and expression studies support this gene as being causative of ANSD.

Conclusions Variants in *AIFM1* gene are a common cause of familial and sporadic ANSD and provide insight into the expanded spectrum of *AIFM1*-associated diseases. The finding of cochlear nerve hypoplasia in some patients was *AIFM1*-related ANSD implies that MRI may be of value in localising the site of lesion and suggests that cochlea implantation in these patients may have limited success.

INTRODUCTION

Auditory neuropathy spectrum disorder (ANSD) is characterised by absent or severely abnormal inner hair cell (IHC) function as measured by auditory brainstem responses (ABRs), with preservation of outer hair cell (OHC) function as indicated by otoacoustic emission (OAE) and/or cochlear microphonic (CM) testing. First described by Starr *et al* in 1996,[1] patients with ANSD present with variable degrees of unilateral or bilateral hearing impairment accompanied by poor speech discrimination and poor word understanding especially in the presence of noise. The prevalence of ANSD varies from 0.5% to 15% among hearing-impaired patients, with an incidence of about 13% in children with severe-to-profound hearing loss.[2–4] Consistent with physiological tests of auditory function, ANSD can be caused by lesions of the IHC, IHC–auditory nerve synapse, auditory nerve or auditory cortex.[5–7]

In many cases of ANSD, the molecular pathology remains unclear, with underlying aetiologies running the gamut of genetic abnormalities, toxic/metabolic derangements, infections, immunological causes and drugs.[8 9] Forty per cent of ANSD is estimated to have a genetic basis with autosomal-dominant, autosomal-recessive, mitochondrial and X-linked inheritance all reported.[3] The list of causative genes includes *OTOF*, *PJVK*, *DIAPH3* and *mtDNA* (*m.1095T>C*) in non-syndromic ANSD and *PMP22*, *MPZ*, *TMEM126A* and *DDDP* in syndromic ANSD, although other genetic aetiologies await discovery.[2]

In 2006, we reported a large Chinese family with X-linked progressive auditory and peripheral sensory neuropathy, and mapped this ANSD locus (AUNX1) to chrXq23-27.3.[10] Using whole-exome sequencing (WES), we have identified the causal AUNX1 gene as *AIFM1* and show that variants in this gene are a common cause of familial and sporadic ANSD. This finding is noteworthy because *AIFM1* mutations are also associated with mitochondrial encephalomyopathy, prenatal ventriculomegaly and Cowchock syndrome, three disorders characterised by developmental disabilities, motor dysfunction, muscle weakness and brain abnormalities as resolved by MRI.[11–13] Our work expands the spectrum of *AIFM1*-associated phenotypes and mandates screening of *AIFM1* in small pedigrees with apparent autosomal-recessive ANSD if X-linked inheritance cannot be excluded.

METHODS

Family ascertainment and clinical evaluation

Five unrelated Chinese families (AUNX1, 7170, 0223, 2724 and 2423) and 93 sporadic male patients diagnosed with ANSD were ascertained through the Department of Otolaryngology, Head

and Neck Surgery, Chinese PLA General Hospital, from November 2000 to June 2014. The phenotype of the AUNX1 family has been reported and includes auditory neuropathy and delayed peripheral sensory neuropathy inherited in an X-linked recessive pattern. The other four families had a similar clinical phenotype. In all cases, genes commonly involved in ANSD such as *OTOF*, *PJVK* and *DIAPH3* were excluded by Sanger sequencing. Acquired causes of ANSD such as prematurity, hyperbilirubinemia, anoxia, hypoxia, congenital brain abnormalities, perinatal intracranial haemorrhage, asphyxia and ototoxic drug exposure were excluded by medical history.

All participants were examined by a multidisciplinary team of healthcare providers that included a neurologist, otolaryngologist and audiologist. The evaluation consisted of a comprehensive medical history, physical examination with careful clinical assessment for peripheral neuropathies, pure-tone audiometry, tympanometry, acoustic reflex testing, ABR, distortion-product OAE testing and electrocochleography. The diagnosis of ANSD was based on recognised criteria (Guidelines Development Conference at NHS 2008, Como, Italy). Neurological examinations included assessments of cranial nerve function, motor activity, muscle weakness, sensory impairment and reflexes. Electrophysiological studies including needle electromyography (EMG), nerve conduction velocity (NCV) and somatosensory evoked potential (SEP) in seven patients from the four unrelated families were carried out. The EMG was performed in the abductor pollicis brevis, tibialis anterior and vastus lateralis muscles. Motor nerve conduction velocities (MCVs) of tibial, peroneal, median and ulnar nerves, as well as sensory nerve conduction velocities (SCVs) of sural, median and ulnar nerves, were obtained. Amplitudes of compound muscle action potential (CMAPs) and sensory nerve action potential (SNAPs) were measured from positive to negative peak values. The Mini Mental State Examination (MMSE) on the three patients (III: 1, III: 9 and III: 11) of family 2423 was conducted to assess the cognitive function. Select patients underwent MRI of brain, temporal high-resolution CT and electrocardiography. Serum enzymes related to energy metabolism, such as lactate dehydrogenase and creatine kinase, were measured.

Peripheral blood samples were obtained and genomic DNA was extracted according to standard procedures. WES was performed on one person from the AUNX1 family (III: 12) and three persons from the 0223 family (II: 1, III: 1 and III: 3). Results were confirmed and validated by Sanger sequencing in these persons and other available family members (figures 1B and 2A). Three other small families (7170, 2724 and 2423, figure 2B–D) and 93 unrelated sporadic cases with ANSD were

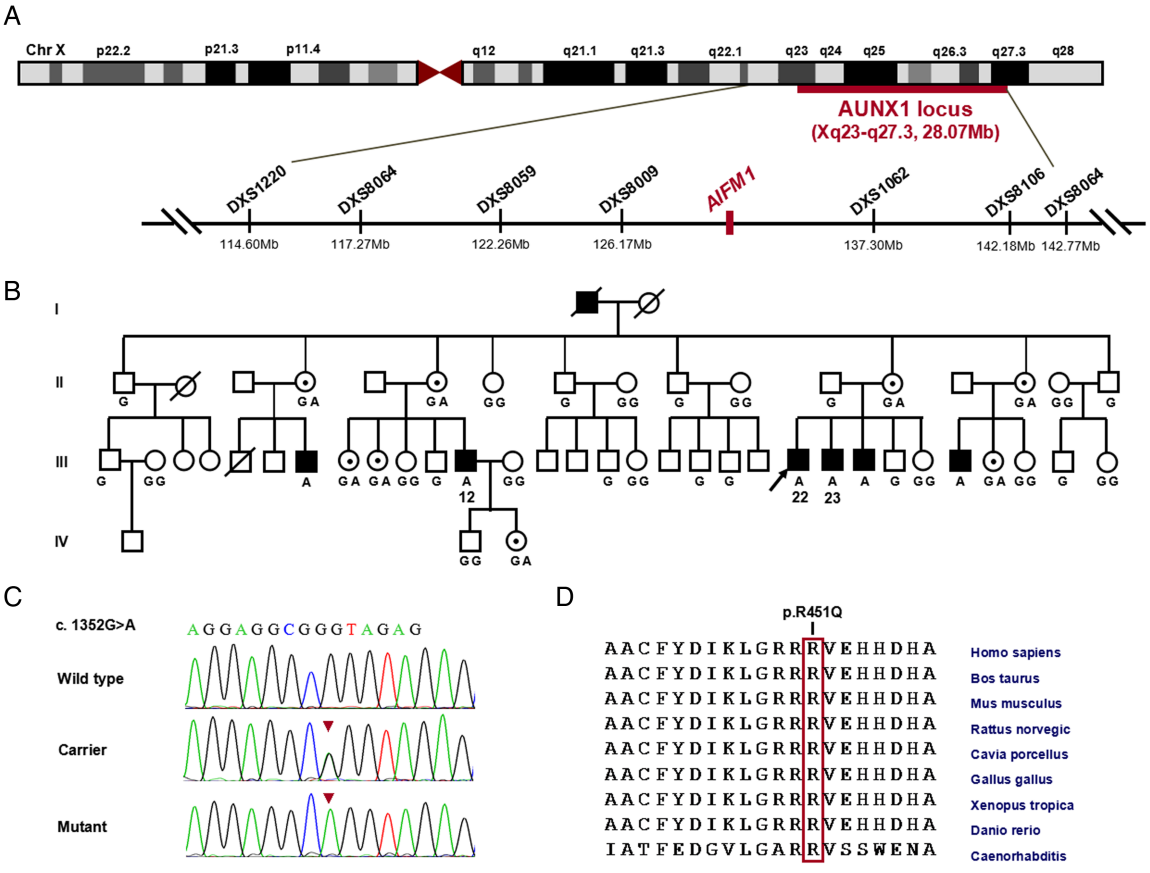

Figure 1 Identification of the disease-causing *AIFM1* mutation in the AUNX1 family segregating auditory and peripheral neuropathy. (A) Schematic genetic and physical map of the AUNX1 locus on chromosome Xq23-q27.3. The location of the *AIFM1* gene is indicated (Mb, million bps). (B) The phenotype in AUNX1 family co-segregates with the c.1352G>A (p.R451Q) mutation in *AIFM1*. The genotypes at c.1352 for the family members are given: G or GG means hemi- or homozygous for the wild-type (WT) sequence, GA means c.1352G>A heterozygous, and A denotes the mutation in hemizygous form. Whole-exome sequencing was completed on subject III: 12. (C) Sequence chromatograms of exon 13 of *AIFM1* show the c.1352G>A (p.R451Q) mutation (arrowhead) in affected males (hemizygote) and female carriers (heterozygote). A homozygous WT sequence is shown on the bottom. (D) Multiple sequence alignment depicts evolutionary conservation of amino acid residue Arg451 (red vertical bar) across human, bovine, mouse, chicken, Xenopus and zebrafish.

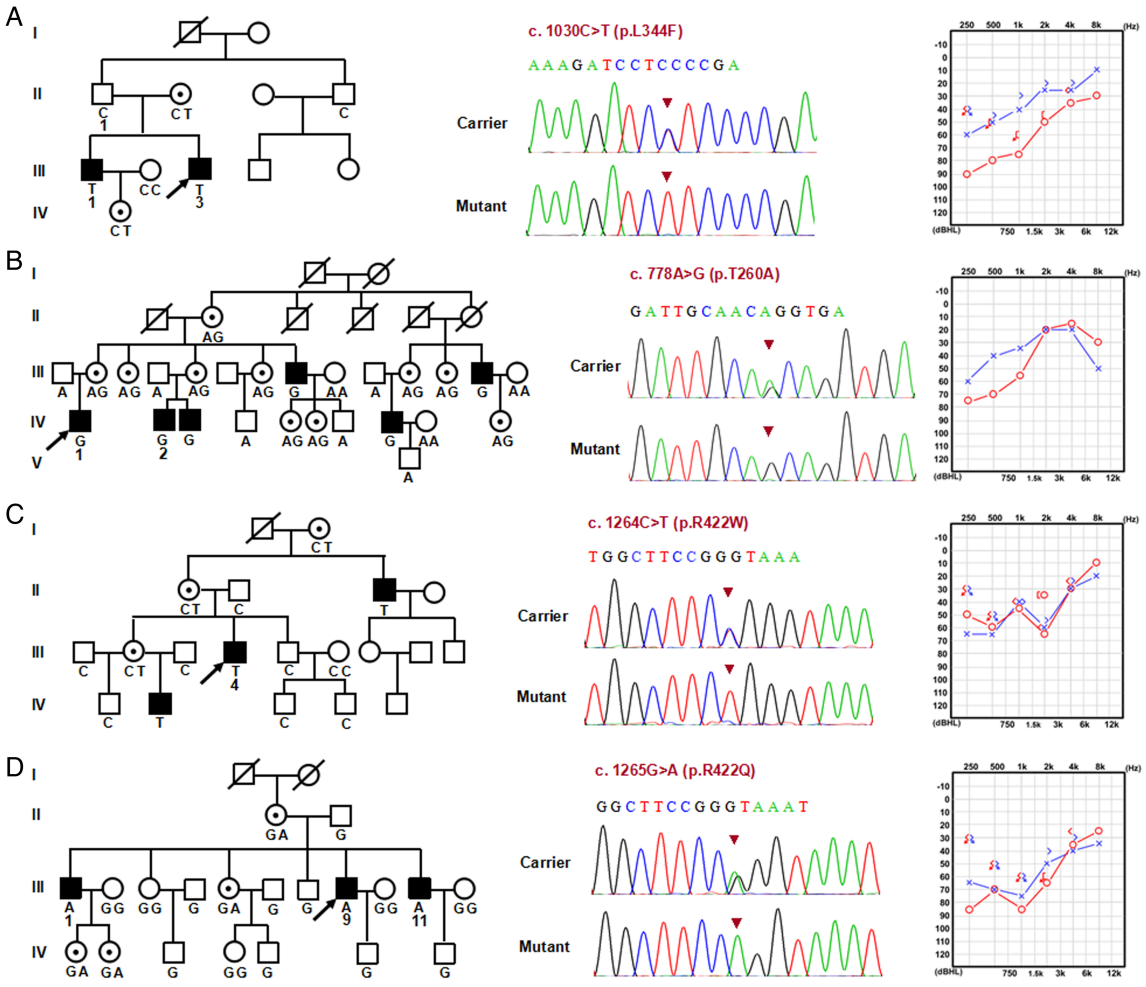

Figure 2 The four auditory neuropathy spectrum disorder families segregating *AIFM1* mutations. Pedigree, sequence results and typical audiogram of each family are shown. Missense mutations c.1030C>T (p.L344F), c.778A>G (p.T260A), c.1264C>T (p.R422W) and c.1265G>A (p.R422Q) were identified in family 0223 (A), 7170 (B), 2724 (C) and 2423 (D), respectively. These mutations co-segregate with auditory and peripheral sensory neuropathy while carriers have normal hearing and sensory ability. The genotypes at c.1030, c.778, c.1264 and c.1265 for the available members in the corresponding family are given respectively. Whole-exome sequencing was completed on three persons in family 0223 (II: 1, III: 1 and III: 3). Needle electromyography and nerve conduction studies were performed on the individuals from family 7170 (IV: 2), family 0223 (III: 3), family 2724 (II: 4) and family 2423 (III: 1, III: 9 and III: 11). The Mini Mental State Examination was conducted on the three patients in family 2423 (III: 1, III: 9 and III: 11).

analysed by Sanger sequencing. Five hundred ethnicity-matched individuals (250 men and 250 women) with normal hearing were recruited as normal controls.

Whole-exome sequencing

Quantified, high-quality genomic DNA (2 μg per person) from one individual from family AUNX1 (III: 12) and three individuals from family 0223 (II: 1, III: 1 and III: 3) was used for WES. Each genomic DNA sample was captured using Agilent SureSelectXT Human All Exon V5 technology (Agilent Technologies, Santa Clara, California, USA) and enriched libraries were sequenced using the HiSeq 2000 platform (Illumina, San Diego, California, USA). Raw image files were processed on the Illumina Pipeline V.1.6 using default parameters, and sequences generated as 75–90 bp paired-end reads were aligned to NCBI37/hg19 assembly. Duplicate reads were removed using Picard (http://picard.sourceforge.net), and clean reads localised to the target region were collected and analysed by SOAPsnp (V.1.03).[14] Local realignment of insertions and deletions (indels) and variant annotation were performed using the Genome Analysis Toolkit (http://www.broadinstitute.org/gatk/).[15] By previously described criteria,[16 17] the low-quality variations were filtered out.

Target enrichment was analysed using NGSrich.[18] Variants were filtered against 1000 Genomes data, and all variants with a minor allele frequency (MAF) >1% were removed from the analysis. Functional annotation of genetic variants was performed using ANNOVAR (http://www.openbioinformatics.org/annovar/). Candidate variants were Sanger validated.

Mutation screening of *AIFM1*

AIFM1 (NC_000023.10) contains 16 exons. Thirty-two primers (16 primer pairs) were designed using Primer V.3.0 software and synthesised by Invitrogen by Life Technology (Beijing, China) to amplify each exon and exon–intron boundaries (see online supplementary table S1). PCR was performed with PE9700 thermocyclers (Applied Biosystems) using standard conditions. Amplified products from all ANSD cases and controls were gel purified and sequenced (ABI 3730, Applied Biosystems). Nucleotide alterations were identified by sequence alignment with the NCBI Reference Sequence (RefSeq) using DNAStar software V.5.0 (DNASTAR, Madison, Wisconsin, USA).

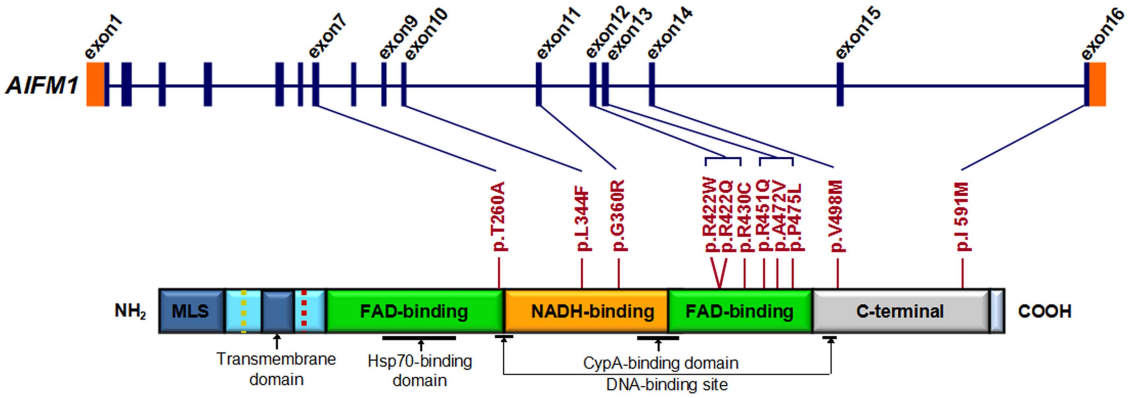

Figure 3 *AIFM1* mutation screening in patients with familial and sporadic auditory neuropathy spectrum disorder (ANSD) with or without peripheral neuropathy. Graphical representation of *AIFM1* structure (upper panel) and its encoded protein (lower panel). *AIFM1* gene has 16 exons. As a flavoprotein with an oxidoreductase enzymatic activity, AIFM1 contains a flavin adenine dinucleotide (FAD)-bipartite domain (in green), a reduced nicotinamide adenine dinucleotide (NADH)-binding motif (in orange) and a C-terminal domain (in grey). It also has a mitochondria localisation sequence (in blue) located in the N-terminal region (reference: http://atlasgeneticsoncology.org//Genes/AIFM1ID44053chXq25.html). The positions of 11 mutations identified in familial and sporadic ANSD cases are shown between the two diagrams (blue lines and red bars). The c.1352G>A (p.R451Q) mutation identified in the AUNX1 family is located in exon 13, which corresponds to the second FAD domain. The longest isoform of *AIFM1* (NM_004208.3; NP_004199.1) was used as the reference sequence for mutation nomenclature.

Evaluation of the pathogenicity

Pathogenicity was assessed using PolyPhen-2 (Polymorphism Phenotyping V.2, http://genetics.bwh.harvard.edu/pph2/index.shtml), SIFT (http://sift.jcvi.org/), Protein Variation Effect Analyzer (PROVEAN) (http://provean.jcvi.org/index.php) and Mutation accessor (http://mutationassessor.org/).

Immunofluorescent staining in mouse inner ear

All experimental procedures were approved by the Institutional Animal Care and Use Committee of the University at Buffalo that conform to the guidelines issued by the National Institutes of Health. Adult mice (C57, 2 months of age) were used for immunofluorescence studies. The cochlear tissues of basilar membrane, spiral ligament and the vestibular end-organ of saccule macula were micro-dissected out as has been described.[19 20] After incubation at 4°C for 24 h with 1% Triton X100 and 5% goat serum in 0.1 M phosphate buffered saline (PBS) containing AIF primary antibody (rabbit monoclonal antibody against AIF, 1:100, Cat# ab32516, Abcam), the specimens were then incubated with tetramethylrhodamine isothiocyanate dextran-conjugated goat antirabbit secondary antibody (1:500, Cat# F6005, Sigma) in PBS for 2 h at room temperature. The speciments were next immersed in Alexa-488-conjugated phalloindin (1:200, Cat#A12379, Invitrogen) for 40 min to label the stereocilia and cuticular plate of the cochlear and vestibular sensory hair cells, and the F-actin in the gap-junction of marginal cells of stria vascularis. The nuclei of tissues were also labelled with 4′,6-diamidino-2-phenylindole dihydrochloride for 30 min. Immunoreactive products were observed under a confocal laser scanning microscope. As a negative control, the primary antibodies were omitted.

RESULTS

Identification of missense mutations in *AIFM1* by WES

To identify the causative variant at the AUNX1 locus, we completed exome sequencing of the proband in family AUNX1. Ninety-nine variants were identified within the AUNX1 locus. After filtering out synonymous changes and variants found in <85% of reads (inconsistent with X-linked inheritance in individual III: 12, an affected man), 24 variants remained: 17 non-synonymous variants, 2 in-frame indels and 5 frameshift indels. Based on incidence data for non-syndromic hearing loss and auditory neuropathy, we excluded variants with an MAF >0.001.[21 22] Three variants remained—*AIFM1* chrX 129267384:G>A; *HS6ST2* chrX 131762528:G>A and *VCX3A* chrX 6452043:C>A—none of which are reported in the NHLBI Go Exome Sequencing Project (ESP) (6503 individuals) or the 1000 Genomes Project (1000G) (1092 individuals). Because *VCX3A* is expressed only in male germ cells, it was not considered further.[23 24] Both of the remaining variants were confirmed in the proband by Sanger sequencing, but only AIFM1 p.R451Q co-segregated with the phenotype in the extended AUNX1 family (eight informative meioses were tested; figure 1A–C). This variant was not found in a screen of 500 normal-hearing ethnicity-matched controls (250 women, 250 men, 750 X chromosomes).

To identify the causative variant in the second family (0223), we completed exome sequencing of the proband (III: 1), his affected brother (III: 3) and unaffected father (II: 1). WES generated an average of 12.3 Gb of sequence, with at least 120× average coverage for each individual as paired-end, 90 bp reads, indicating the high quality of sequencing (see online supplementary figures S1 and S2 and table S2). After mapping to the reference genome sequence, >99.0% of the targeted bases were covered sufficiently to pass quality assessment for calling single-nucleotide polymorphisms (SNPs) and short indels (see online supplementary table S2). We identified an average of ~20 700 SNPs in coding regions (exonic), an average of 129 variants (SNPs and indels) within 2 bp of an exon/intron boundary that may affect splicing, and an average of 1270 indels in coding regions (see online supplementary table S3). Because the two affected individuals share the causal variant when compared with their normal-hearing father, a total of 807 variants were retained after filtering against SNP and Indel databases including dbSNP 141, 1000G, Hapmap 8 and YH (see online supplementary tables S4 and S5). Among them, 213 variants (including 129 non-synonymous SNPs and splice sites, as well as 84 indels) were predicted to have a functional impact (see online supplementary tables S6 and S7). Because inheritance was consistent with an autosomal or X-linked recessive pattern based on family pedigrees, candidate pathogenic variants selected for further

Table 1 Summary of the clinical phenotypes for cases with AIFM1 mutations

Cases ID	7170*	0223*	1302	1757	7187	1747	2724*	3033	6962	2423*	0077	AUNX1*	1806	0046	4678	3305
Mutation† detected	c.778A>G (p.T260A)	c.1030C>T (p.L344F)‡				c.1078G>C (p.G360R)	c.1264C>T (p.R422W)§			c.1265G>A (p.R422Q)	c.1288C>T (p.R430C)	c.1352G>A (p.R451Q)	c.1415C>T (p.A472V)	c.1424C>T (p.P475L)	c.1492G>A (p.V498M)	c.1773C>G (p.I591M)
Hearing loss degree¶	Mild	Mild	Mild	Mild	Moderate	Moderate	Moderate	Mild	Mild	Moderate	Mild	Moderate	Mild	Moderate	Moderate	Mild
Tinnitus	+	–	+	+	+	+	+	+	–	+	–	+	+	–	+	+
Vertigo	–	–	–	–	–	–	–	–	–	–	–	–	–	–	–	–
Unsteadiness	+	+	–	–	–	+	+	+	–	+	–	+	–	–	–	–
Numbness of extremities	+	+	–	+	–	+	+	+	–	+	–	+	–	–	–	–
Visual impairment	–	–	–	–	–	Myopia	–	–	–	Myopia	–	–	Myopia	–	–	Myopia
Foot deformity	–	–	–	–	–	–	–	–	–	–	–	–	–	–	–	–
Muscle atrophy	–	–	–	–	–	–	–	–	–	–	–	–	–	–	–	–
Intellectual abilities	–	–	–	–	–	–	–	–	–	–	–	–	–	–	–	–
MRI of brain	CNH	CNH	NT	NT	CNH	NT	CNH	NT	NT	CNH	NT	CNH	NT	NT	NT	CNH
CT of temporal bone	–	–	NT	NT	–	NT	–	–	–	–	NT	–	NT	NT	NT	–

*Familial cases, representing the probands of the AN families. The other cases are sporadic cases.
†RefSeq: NM_004208.3, NP_ NP_004199.1, GRCh38/hg38 chrX: NC_000023.11 (130129362..130165887, complement).
‡The mutation of c.1030C>T (p.L344F) was detected not only in family 0223 but also in other three sporadic cases 1302, 1757 and 7187.
§The mutation of c.1264C>T (p.R422W) was detected not only in family 2724 but also in the two sporadic cases 3033 and 6962.
¶The degrees of hearing loss were evaluated based on the recommendations of the EU HEAR project, as described by Stephens (2001), and the detailed audiological data of the auditory neuropathy spectrum disorder cases are summarised in online supplementary table S9.
+/–, positive or negative finding; CNH, cochlear nerve hypoplasia; NT, not tested.

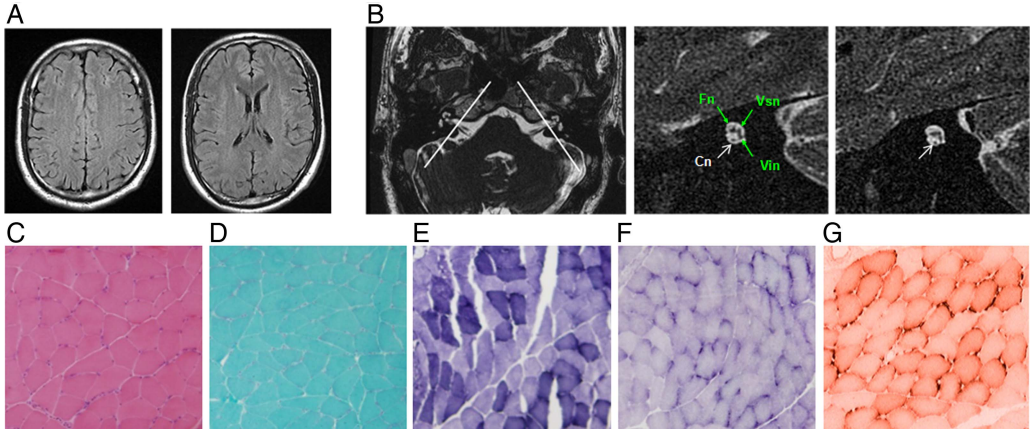

Figure 4 Brain MRI imaging and muscle biopsy immune-staining of the patient (III: 3) from family 0223. (A) Serial cerebral MRI with fluid-attenuated inversion recovery sequence demonstrates normal signal intensity in bilateral centrum semiovale (left panel) and periventricular and subcortical white matter (right panel). (B) Axial view of the cerebellopontine angle and the internal auditory canal (IAC) shows normal anatomy (left panel). The two white lines illustrate the plane prescribed for oblique plane sagittal images obtained perpendicular to the nerves of the IAC. The oblique plane sagittal image (3D-fast-spin echo sequence, middle panel) obtained on the left side demonstrates an abnormally small cochlea nerve (Cn, white arrow) but a normal size IAC with normal facial (Fn), superior (Vsn) and inferior (Vin) vestibular nerves (green arrows). The right Cn was symmetrically small (right panel, white arrow). (C–F) Immunohistochemical staining of muscle biopsy (left gastrocnemius) in patient III: 3 shows a few atrophic myofibers (H&E, C). No ragged red fibres (modified Gomori-trichrome, D), ragged blue fibres (succinate dehydrogenase, E) or targetoid fibres (nicotinamide adenine dinucleotide-tetrazolium reductase, F) are identified. There is no reduction or absence of cytochrome-*c*-oxidase histochemical reactions observed (G).

analysis were rare homozygous or hemizygous nonsense, missense, splice site and indel variants with allele frequencies of ≤0.005 in public variant databases. Combined with the predicted effect on protein function by SIFT, PolyPhen2 and Mutation Assessor programs, we identified five variants (including one rare SNP and four indels) to be candidates (see online supplementary table S8). After Sanger sequencing and genotyping in all available family members, the only variant segregating with the phenotype (auditory and peripheral sensory neuropathy) of family 0223 was c.1030C>T (p.L344F) in the AIFM1 gene (figure 2A). This variant is recorded in dbSNP (rs184474885, http://www.ncbi.nlm.nih.gov/projects/SNP) with a very low MAF (A=0.0005, 2/3775). Interestingly, although this variant is recorded as an SNP in 1000G, it was not found in the screen of 500 normal-hearing ethnicity-matched controls in Chinese populations (mentioned above).

Mutation spectrum of *AIFM1* in familial and sporadic ANSD

To investigate the contribution of *AIFM1* to ANSD in China, we screened this gene for mutations in our extended familial and sporadic ANSD cohort; identifying 10 more novel missense mutations in three additional families and 11 of 93 (10%) men with an ANSD phenotype (figure 3, table 1 and online supplementary table S9). In all cases of familial ANSD, the identified missense mutations (c.778A>G [p.T260A], c.1030C>T [p.L344F], c.1264C>T [p.R422W], c.1265G>A [p.R422Q], c.1352G>A [p.R451Q]) completely segregated with the auditory and peripheral sensory neuropathy phenotype, with female carriers not reporting any signs of ANSD or peripheral sensory neuropathy (figures 1B and 2). Two variants identified in familial ANSD, c.1030C>T (p.L344F) and c.1264C>T (p.R422W), were also detected in sporadic ANSD cases, with similar phenotypes (table 1). All of the 10 additional *AIFM1* mutations were also absent in the screen of normal-hearing ethnicity-matched controls (750 X chromosomes). None of these variants were found in ESP or 1000G except c.1030C>T (p.L344F) (see online supplementary table S10).

Clinical manifestations of *AIFM1*-associated ANSD

The phenotype associated with the AUNX1-causing *AIFM1* p.R451Q mutation is characterised by childhood-onset ANSD and delayed peripheral sensory neuropathy presenting as extremity numbness, unsteadiness and areflexia.[25] This clinical picture was seen with the other familial cases of *AIFM1* ANSD (0223, 7170, 2724 and 2423) and in some patients with sporadic *AIFM1* ANSD (table 1 and online supplementary table S9). The electrophysiological findings of 14 nerves in seven affected familial members were obtained (see online supplementary table S11). Nerve conduction studies demonstrated reduced sural, median and ulnar sensory NCVs or even absent responses. The reduced SCVs were always associated with reduced SNAPs (see online supplementary figure S3). The abnormal SEP results were also recorded, including no response or prolonged latency for the evoked potential P40 of tibial SEP, with or without prolonged latency of N9 potential of median SEP (see online supplementary figure S4). The data indicated that the patients might have demyelination changes in the peripheral sensory nerves. However, the MCVs and CMAPs of all patients were normal (see online supplementary figure S3). Needle EMG performed in these patients also showed normal values. There were no fibrillation, positive or fasciculation potentials and myotonic discharges were not observed. The patients also showed normal motor unit action potentials (see online supplementary figure S5). All of these findings suggested that the affected patients had evidence of peripheral sensory neuropathy but not motor neuropathy nor myopathy. The MMSE scores of patients III: 1, III: 9 and III: 11 from family 2423 were in the normal range (27–30): 28, 27 and 28, respectively with their corresponding educational backgrounds of junior college, high school and middle school. These normal scores (≥27) indicated normal cognitive function.

Re-examination of patients showed that both hearing impairment and sensory neuropathy slowly progress.[10 25] Although serial cerebral MRI in familial ANSD demonstrated normal signal intensity in the brain, inclined sagittal MRI of the internal auditory canals showed bilateral cochlea nerve hypoplasia

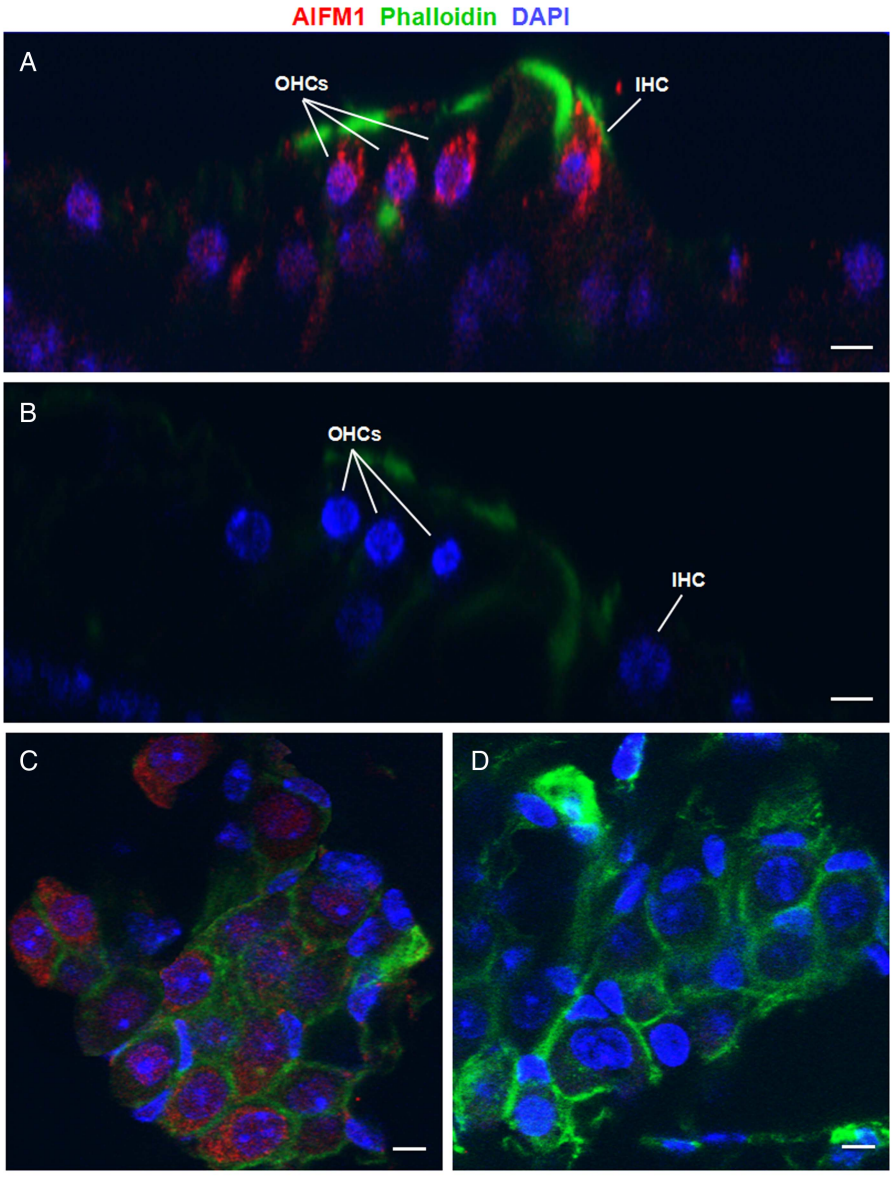

Figure 5 Localisation of AIFM1 in the murine inner ear by immunostaining with a monoclonal AIFM1 antibody. (A) Organ of Corti whole-mount preparation demonstrates AIFM1 (red) localisation to the cytoplasm of inner hair cell (IHC) and outer hair cells (OHCs), as well as the surrounding tissue. (B) Control organ of Corti tissue labelled with only secondary antibody and phalloidin (green). (C) Spiral ganglion whole-mount preparation shows AIFM1 (red) staining in spiral ganglion neurons. (D) Control spiral ganglion tissue labelled with secondary antibody and phalloidin (green). The scale bar indicates 15 μm in panels A and B, and 10 μm in panels C and D. DAPI, 4′,6-diamidino-2-phenylindole dihydrochloride.

(CNH), a finding consistent with the diagnosis of ANSD (figure 4A, B and table 1). No symptoms or signs of muscle wasting, weakness or atrophy were identified in *AIFM1* mutated patients, and muscle biopsy of the left gastrocnemius in an affected member of family 0223 (III: 2) revealed only a few atrophic myofibers (figure 4C–G). All patients with *AIFM1* mutations had normal serum levels of lactate dehydrogenase and creatine kinase.

Impact on protein structure

We evaluated the functional effects of the 11 amino acid substitutions identified in this study using Polyphen2, SIFT, PROVEAN and Mutation Assessor.[26–30] Nine variants were predicted to be likely pathogenic by at least three programs. (We considered the following predictions as pathogenic: Polyphen2, probably damaging; SIFT, damaging; PROVEA, deleterious; Mutation Assessor, medium/high functional impact). The exceptions, p.R422Q and p.I591M, were predicted pathogenic by two and one program, respectively (figure 3 and online supplementary table S12). Structural comparison of wild-type versus mutated AIFM1 protein showed that mutations in the two flavin adenine dinucleotide (FAD) and reduced nicotinamide adenine dinucleotide (NADH) domains have greater impact on the protein surface than mutations in C-terminus (see online supplementary figures S6 and S7).

Histological findings

Immunostaining of murine inner ear demonstrated ubiquitous localisation of AIFM1 in the inner, especially to the cytoplasm of IHC, OHCs and spiral ganglion neurons, consistent with a role in normal auditory function (figure 5 and online supplementary figures S8–S9).

DISCUSSION

In 2006, we mapped a novel X-linked auditory neuropathy locus (AUNX1) to chrXq23-q27.3 in a large five-generation Chinese family.[10] Using WES and confirmatory segregation analysis, we now report a novel missense change, p.R451Q in *AIFM1*, as causally responsible for the phenotype in this family. Consistent with its playing a major role in ANSD, we have identified 10 other mutations in *AIFM1* in a cohort of familial and sporadic cases of ANSD of Chinese ethnicity. In all familial cases, the identified variants (p.T260A, p.L344F, p.R422W and p.R422Q) co-segregate with the auditory and peripheral sensory

neuropathy. All 11 variants were absent in a screen of 500 normal-hearing, ethnicity-matched Chinese controls (750 X chromosomes) and 9 were classified as likely damaging by multiple bioinformatics programs (see online supplementary table S12). In aggregate, these data provide abundant compelling evidence to implicate *AIFM1* in X-linked recessive ANSD.

AIFM1 encodes apoptosis-inducing factor 1, a flavoprotein located in the mitochondrial intermembrane space. AIFM1 has at least two functions.[31–33] First, as a caspase-independent death effector, it mediates caspase-independent programmed cell death when translocating from mitochondria to the nucleus upon apoptotic stimuli. And second, as an FAD-dependent NADH oxidoreductase, it plays an important role in oxidative phosphorylation, redox control and respiratory chain activity in healthy cells. To date, *AIFM1* mutations have been associated with a severe mitochondrial encephalomyopathy (COXPD6, MIM# 300816; caused by p.R201del),[11] prenatal ventriculomegaly (caused by p.G308E)[12] and Cowchock syndrome (CMTX4, MIM# 310490; caused by p.E493V).[13] Common features of these disorders are developmental disabilities such as mental retardation, motor dysfunction and muscle weakness, and abnormal MRI findings in brain.[11–13] The AUNX1 phenotype is very different from these other phenotypes, as is the location of the causal mutations in the protein (see online supplementary table S13 and figure S10).

Based on phenotypic variability, it has been suggested that AIFM-related diseases have differing pathogenic mechanisms.[34] In Cowchock syndrome, the p.E493V mutation alters the redox properties of the mutated protein, resulting in increased apoptosis.[13] In COXPD6, in comparison, the R201del mutation reduces activity of respiratory chain complexes I–V and increases caspase-independent programmed cell death.[11] Most of the 11 mutations identified in this study are located in the NADH and second FAD domains of AIFM1, which are essential for FAD-dependent NADH oxidoreductase.

Interestingly, in spite of the widespread expression of AIFM1 in murine inner ear, which is consistent with a role in normal auditory function, the mutated protein did not affect OHCs function as measured by distortion product otoacoustic emission responses (figure 5 and online supplementary table S9). In addition, while some patients with *AIFM1* mutations had MRI-documented CNH, the onset of hearing problems was typically during adolescence, suggesting that the hypoplasia represents late-onset and not congenital degeneration (see online supplementary figure S10; table 1).[35 36]

ANSD is known to be an extremely complex disease that has congenital and acquired forms. Extensive clinical testing and genetic research are invaluable to elucidate underlying mechanisms and sites of pathology.[37–39] Our finding of bilateral CNH in *AIFM1*-related ANSD implies that MRI screening may identify the site of lesion in some patients with this phenotype. Furthermore, it suggests that if CNH is an eventual common outcome cochlea implantation in patients with *AIFM1*-related ANSD may meet with limited success.[40–42] In most patients, we were able to diagnose the other aspect of the phenotype, peripheral sensory neuropathy, by clinical and neurophysiological testing, although the symptoms of sensory neuropathy may occur many months or even years after the auditory neuropathy (see online supplementary table S11).

In conclusion, our study identifies *AIFM1* as a new causal gene associated with X-linked auditory neuropathy and delayed peripheral neuropathy. These results expand the spectrum of *AIFM1*-associated diseases to include ANSD. Because female carriers are unaffected, *AIFM1* should be considered in small pedigrees with apparent autosomal recessive ANSD if X-linked inheritance cannot be excluded. Further studies are required to determine the long-term benefit these patients may receive from cochlear implantation.

Author affiliations
[1]Department of Otolaryngology-Head and Neck Surgery, Institute of Otolaryngology, PLA General Hospital, Beijing, China
[2]Molecular Otolaryngology and Renal Research Laboratories and the Department of Otolaryngology-Head and Neck Surgery, University of Iowa, Iowa City, Iowa, USA
[3]Department of Otolaryngology-Head & Neck Surgery, Stanford University School of Medicine, Stanford, California, USA
[4]Beijing Institute of Otorhinolaryngology, Beijing Tongren Hospital, Capital Medical University, Beijing, China
[5]National Institute of Biological Sciences, Beijing, China
[6]Department of Communicative Disorders & Sciences, Center for Hearing and Deafness, University at Buffalo, Buffalo, New York, USA
[7]Department of Radiology, PLA General Hospital, Beijing, China
[8]Department of Neurology, PLA General Hospital, Beijing, China
[9]Key Laboratory of Mental Health, Institute of Psychology, Chinese Academy of Sciences, Beijing, China
[10]BGI-Shenzhen, Shenzhen, China
[11]Unité de Génétique et Physiologie de l'Audition, Institut Pasteur, Collège de France, Paris, France

Acknowledgements We would like to thank the families and the patients for their invaluable cooperation and participation. We thank Chao Zhang and Lan Yu for auditory testing in patients, Cui Zhao and Na Li for collecting and preparing DNA samples, Nan Liu for assistance with PCR and Sanger sequencing.

Contributors The first three authors (LZ, JG, ME) contributed equally to this work. Performed the experiments: LZ, JG, ME, QZ, YZ, ZS, FW, JY, CB, WS, LL, DD, LX, YQ, QS and WX. Contributed reagents/materials/analysis tools: DW, HW, WS, DD, XL, XH, DW, SC, ZY, NY, JuW and JiW. Wrote the paper: QW, LZ and RJHS. Critical reading and discussion of manuscript: QW, RJHS, RJS and CP. QW and RJHS are guarantors responsible for this work.

Funding This study was financially supported by the National Key Basic Research Program of China (no. 2014CB943001) and the National Natural Science Foundation of China, Major Project (no. 81120108009) to QW; and the National Institutes of Health (NIDCD DC003544, DC002842 and DC012049 to RJHS). The funders had no role in study design, data collection and analysis, decision to publish or preparation of the manuscript.

Competing interests None declared.

Patient consent Obtained.

Ethics approval The Ethics Reviewing Committee of the Chinese PLA General Hospital.

Provenance and peer review Not commissioned; externally peer reviewed.

REFERENCES

1 Starr A, Picton TW, Sininger Y, Hood LJ, Berlin CI. Auditory neuropathy. *Brain* 1996;119:741–53.
2 Manchaiah VK, Zhao F, Danesh AA, Duprey R. The genetic basis of auditory neuropathy spectrum disorder (ANSD). *Int J Pediatr Otorhinolaryngol* 2011;75:151–8.
3 Del Castillo FJ, Del Castillo I. Genetics of isolated auditory neuropathies. *Front Biosci (Landmark Ed)* 2012;17:1251–65.
4 Sanyelbhaa Talaat H, Kabel AH, Samy H, Elbadry M. Prevalence of auditory neuropathy (AN) among infants and young children with severe to profound hearing loss. *Int J Pediatr Otorhinolaryngol* 2009;73:937–9.
5 El-Badry MM, McFadden SL. Evaluation of inner hair cell and nerve fiber loss as sufficient pathologies underlying auditory neuropathy. *Hear Res* 2009;255:84–90.
6 Giraudet F, Avan P. Auditory neuropathies: understanding their pathogenesis to illuminate intervention strategies. *Curr Opin Neurol* 2012;25:50–6.
7 Ngo RY, Tan HK, Balakrishnan A, Lim SB, Lazaroo DT. Auditory neuropathy/auditory dys-synchrony detected by universal newborn hearing screening. *Int J Pediatr Otorhinolaryngol* 2006;70:1299–306.
8 Beutner D, Foerst A, Lang-Roth R, von Wedel H, Walger M. Risk factors for auditory neuropathy/auditory synaptopathy. *ORL J Otorhinolaryngol Relat Spec* 2007;69:239–44.

9 Declau F, Boudewyns A, Van den Ende J, van de Heyning P. Auditory neuropathy: a challenge for diagnosis and treatment. *B-ENT* 2013;Suppl 21:65–79.
10 Wang QJ, Li QZ, Rao SQ, Lee K, Huang XS, Yang WY, Zhai SQ, Guo WW, Guo YF, Yu N, Zhao YL, Yuan H, Guan J, Leal SM, Han DY, Shen Y. AUNX1, a novel locus responsible for X linked recessive auditory and peripheral neuropathy, maps to Xq23-27.3. *J Med Genet* 2006;43:e33.
11 Ghezzi D, Sevrioukova I, Invernizzi F, Lamperti C, Mora M, D'Adamo P, Novara F, Zuffardi O, Uziel G, Zeviani M. Severe X-linked mitochondrial encephalomyopathy associated with a mutation in apoptosis-inducing factor. *Am J Hum Genet* 2010;86:639–49.
12 Berger I, Ben-Neriah Z, Dor-Wolman T, Shaag A, Saada A, Zenvirt S, Raas-Rothschild A, Nadjari M, Kaestner KH, Elpeleg O. Early prenatal ventriculomegaly due to an AIFM1 mutation identified by linkage analysis and whole exome sequencing. *Mol Genet Metab* 2011;104:517–20.
13 Rinaldi C, Grunseich C, Sevrioukova IF, Schindler A, Horkayne-Szakaly I, Lamperti C, Landouré G, Kennerson ML, Burnett BG, Bönnemann C, Biesecker LG, Ghezzi D, Zeviani M, Fischbeck KH. Cowchock syndrome is associated with a mutation in apoptosis-inducing factor. *Am J Hum Genet* 2012;91:1095–102.
14 Li R, Li Y, Fang X, Yang H, Wang J, Kristiansen K, Wang J. SNP detection for massively parallel whole-genome resequencing. *Genome Res* 2009;19:1124–32.
15 McKenna A, Hanna M, Banks E, Sivachenko A, Cibulskis K, Kernytsky A, Garimella K, Altshuler D, Gabriel S, Daly M, DePristo MA. The Genome Analysis Toolkit: a MapReduce framework for analyzing next-generation DNA sequencing data. *Genome Res* 2010;20:1297–303.
16 Zhao Y, Zhao F, Zong L, Zhang P, Guan L, Zhang J, Wang D, Wang J, Chai W, Lan L, Li Q, Han B, Yang L, Jin X, Yang W, Hu X, Wang X, Li N, Li Y, Petit C, Wang J, Wang HY, Wang Q. Exome sequencing and linkage analysis identified tenascin-C (TNC) as a novel causative gene in nonsyndromic hearing loss. *PLoS One* 2013;8: e69549.
17 Azaiez H, Booth KT, Bu F, Huygen P, Shibata SB, Shearer AE, Kolbe D, Meyer N, Black-Ziegelbein EA, Smith RJ. TBC1D24 mutation causes autosomal-dominant nonsyndromic hearing loss. *Hum Mutat* 2014;35:819–23.
18 Frommolt P, Abdallah AT, Altmüller J, Motameny S, Thiele H, Becker C, Stemshorn K, Fischer M, Freilinger T, Nürnberg P. Assessing the enrichment performance in targeted resequencing experiments. *Hum Mutat* 2012;33:635–41.
19 Ding D, He J, Allman BL, Yu D, Jiang H, Seigel GM, Salvi RJ. Cisplatin ototoxicity in rat cochlear organotypic cultures. *Hear Res* 2011;282:196–203.
20 Ding D, Qi W, Yu D, Jiang H, Han C, Kim MJ, Katsuno K, Hsieh YH, Miyakawa T, Salvi R, Tanokura M, Someya S. Addition of exogenous NAD+ prevents mefloquine-induced neuroaxonal and hair cell degeneration through reduction of caspase-3-mediated apoptosis in cochlear organotypic cultures. *PLoS One* 2013;8: e79817.
21 Korver AM, van Zanten GA, Meuwese-Jongejeugd A, van Straaten HL, Oudesluys-Murphy AM. Auditory neuropathy in a low-risk population: a review of the literature. *Int J Pediatr Otorhinolaryngol* 2012;76:1708–11.
22 Shearer AE, Eppsteiner RW, Booth KT, Ephraim SS, Gurrola J, Simpson A, Black-Ziegelbein EA, Joshi S, Ravi H, Giuffre AC, Happe S, Hildebrand MS, Azaiez H, Bayazit YA, Erdal ME, Lopez-Escamez JA, Gazquez I, Tamayo ML, Gelvez NY, Leal GL, Jalas C, Ekstein J, Yang T, Usami S, Kahrizi K, Bazazzadegan N, Najmabadi H, Scheetz TE, Braun TA, Casavant TL, LeProust EM, Smith RJH. Utilizing ethnic-specific differences in minor allele frequency to re-categorize reported pathogenic deafness variants. *Am J Hum Genet* 2014;95:445–53.
23 Fukami M, Kirsch S, Schiller S, Richter A, Benes V, Franco B, Muroya K, Rao E, Merker S, Niesler B, Ballabio A, Ansorge W, Ogata T, Rappold GA. A member of a gene family on Xp22.3, VCX-A, is deleted in patients with X-linked nonspecific mental retardation. *Am J Hum Genet* 2000;67:563–73.
24 Lahn BT, Page DC. A human sex-chromosomal gene family expressed in male germ cells and encoding variably charged proteins. *Hum Mol Genet* 2000;9:311–19.
25 Wang Q, Gu R, Han D, Yang W. Familial auditory neuropathy. *Laryngoscope* 2003;113:1623–9.
26 Adzhubei IA, Schmidt S, Peshkin L, Ramensky VE, Gerasimova A, Bork P, Kondrashov AS, Sunyaev SR. A method and server for predicting damaging missense mutations. *Nat Methods* 2010;7:248–9.
27 Kumar P, Henikoff S, Ng PC. Predicting the effects of coding non-synonymous variants on protein function using the SIFT algorithm. *Nat Protoc* 2009;4:1073–81.
28 Choi Y, Sims GE, Murphy S, Miller JR, Chan AP. Predicting the Functional Effect of Amino Acid Substitutions and Indels. *PLoS ONE* 2012;7:e46688.
29 Reva B, Antipin Y, Sander C. Determinants of protein function revealed by combinatorial entropy optimization. *Genome Biol* 2007;8:R232.
30 Reva B, Antipin Y, Sander C. Predicting the functional impact of protein mutations: application to cancer genomics. *Nucleic Acids Res* 2011;39:e118.
31 Hangen E, Blomgren K, Bénit P, Kroemer G, Modjtahedi N. Life with or without AIF. *Trends Biochem Sci* 2010;35:278–87.
32 Norberg E, Orrenius S, Zhivotovsky B. Mitochondrial regulation of cell death: processing of apoptosis-inducing factor (AIF). *Biochem Biophys Res Commun* 2010;396:95–100.
33 Polster BM. AIF, reactive oxygen species, and neurodegeneration: a "complex" problem. *Neurochem Int* 2013;62:695–702.
34 Delavallée L, Cabon L, Galán-Malo P, Lorenzo HK, Susin SA. AIF-mediated caspase-independent necroptosis: a new chance for targeted therapeutics. *IUBMB Life* 2011;63:221–32.
35 Roche JP, Huang BY, Castillo M, Bassim MK, Adunka OF, Buchman CA. Imaging characteristics of children with auditory neuropathy spectrum disorder. *Otol Neurotol* 2010;31:780–8.
36 Young NM, Kim FM, Ryan ME, Tournis E, Yaras S. Pediatric cochlear implantation of children with eighth nerve deficiency. *Int J Pediatr Otorhinolaryngol* 2012;76:1442–8.
37 Santarelli R. Information from cochlear potentials and genetic mutations helps localize the lesion site in auditory neuropathy. *Genome Med* 2010;2:91.
38 Vlastarakos PV, Nikolopoulos TP, Tavoulari E, Papacharalambous G, Korres S. Auditory neuropathy: endocochlear lesion or temporal processing impairment? Implications for diagnosis and management. *Int J Pediatr Otorhinolaryngol* 2008;72:1135–50.
39 Rapin I, Gravel J. "Auditory neuropathy": physiologic and pathologic evidence calls for more diagnostic specificity. *Int J Pediatr Otorhinolaryngol* 2003;67:707–28.
40 Kutz JW Jr, Lee KH, Isaacson B, Booth TN, Sweeney MH, Roland PS. Cochlear implantation in children with cochlear nerve absence or deficiency. *Otol Neurotol* 2011;32:956–61.
41 Glastonbury CM, Davidson HC, Harnsberger HR, Butler J, Kertesz TR, Shelton C. Imaging findings of cochlear nerve deficiency. *AJNR Am J Neuroradiol* 2002;23:635–43.
42 Valero J, Blaser S, Papsin BC, James AL, Gordon KA. Electrophysiologic and behavioral outcomes of cochlear implantation in children with auditory nerve hypoplasia. *Ear Hear* 2012;33:3–18.

Figure S1 The distribution of per-base sequencing depth in target regions for each sample in family 0223. Y-axis indicated the percentage of total target region under a given sequencing depth.

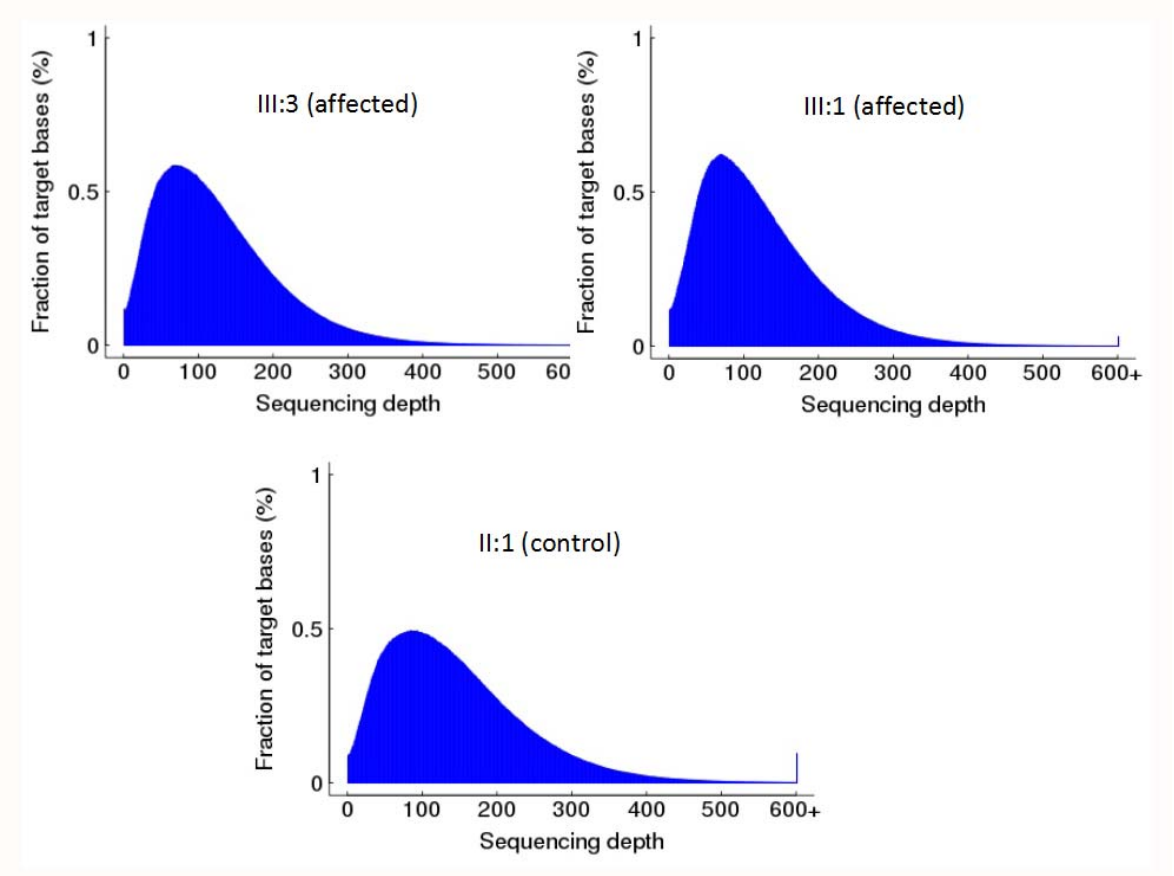

Figure S2 Cumulative depth distribution in target regions for each sample in family 0223. X-axis denotes sequencing depth, and Y-axis indicated the fraction of bases that achieves at or above a given sequencing depth.

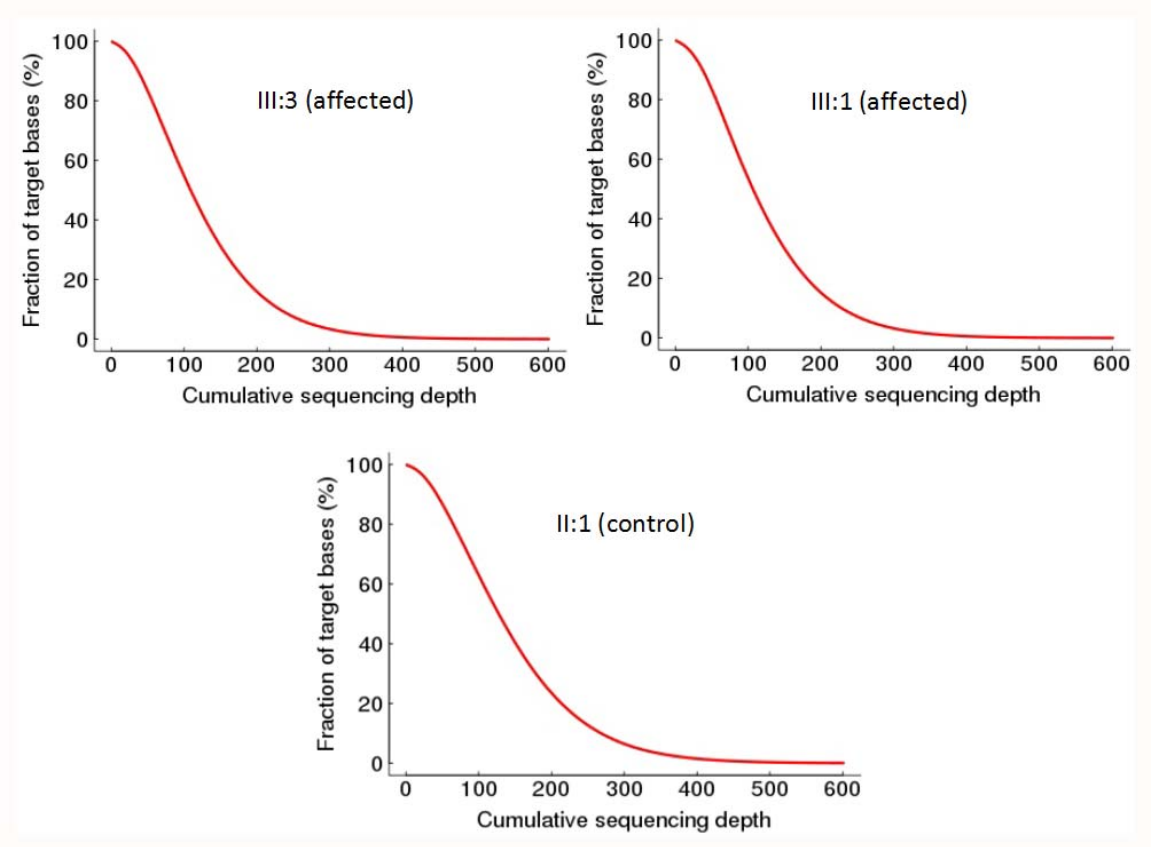

Figure S3 The CVs recordings in patient III: 9 of family 2423. The SCV of left suralis showed no response (upper panel). The MCV of left Peroneus was in normal range (lower panel).

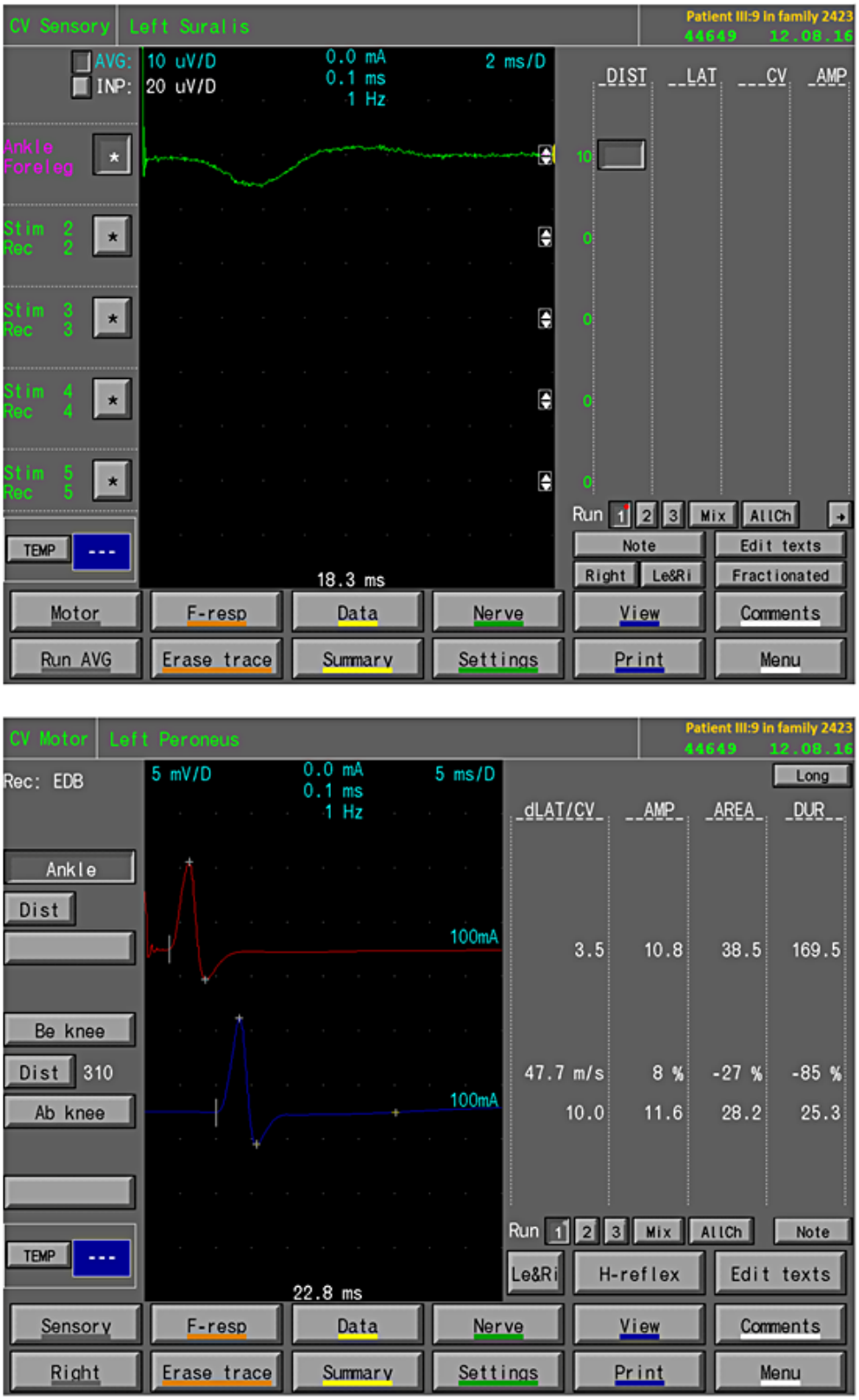

Figure S4 The SEP recordings in patient III: 9 of family 2423. Left tibial SEP at ankle showed no response for the evoked potential P40 (upper panel). Left median SEP at wrist showed prolonged latency of N9 potential (lower panel).

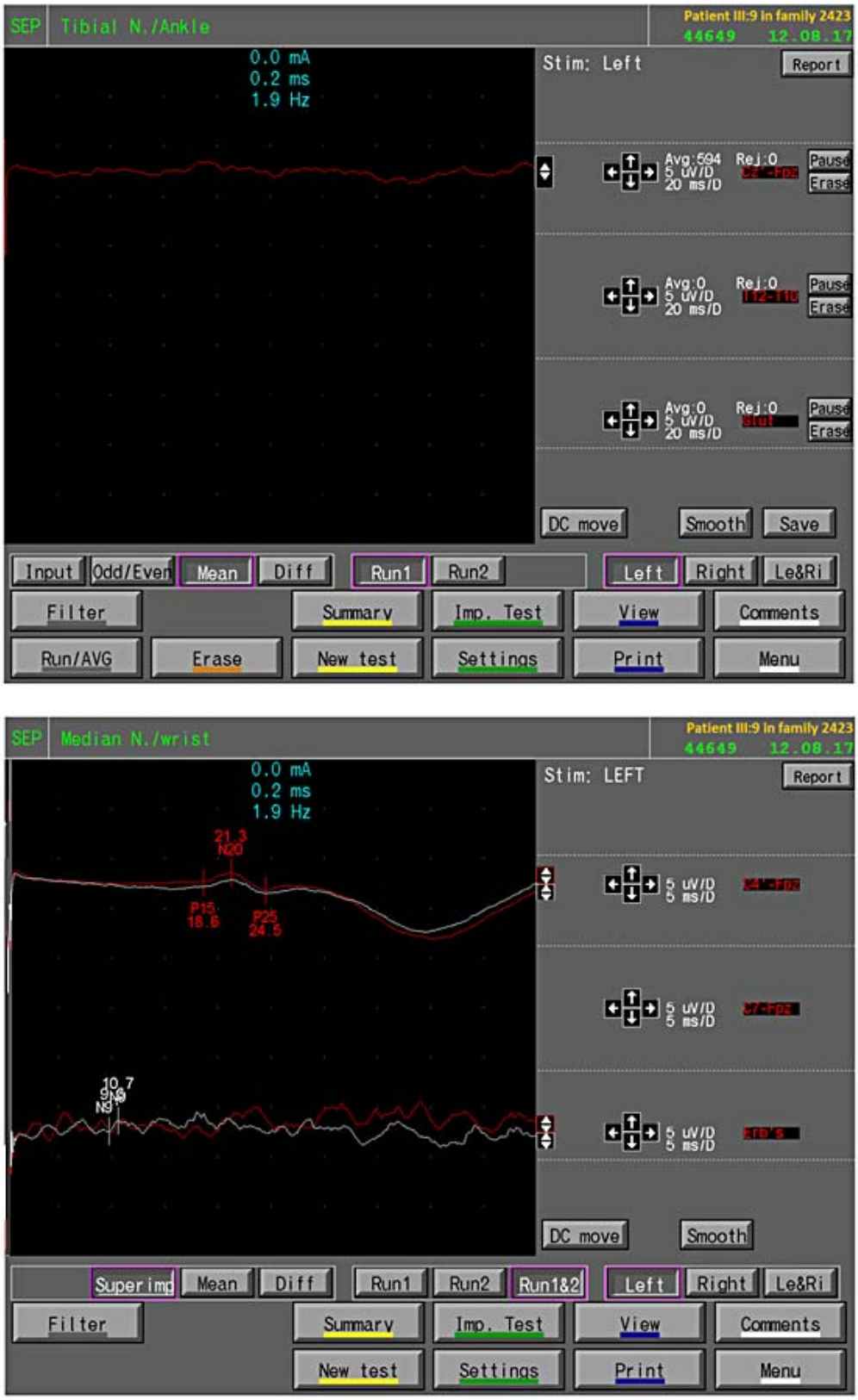

Figure S5 Normal MUPs recordings of patient III: 9 of family 2423.

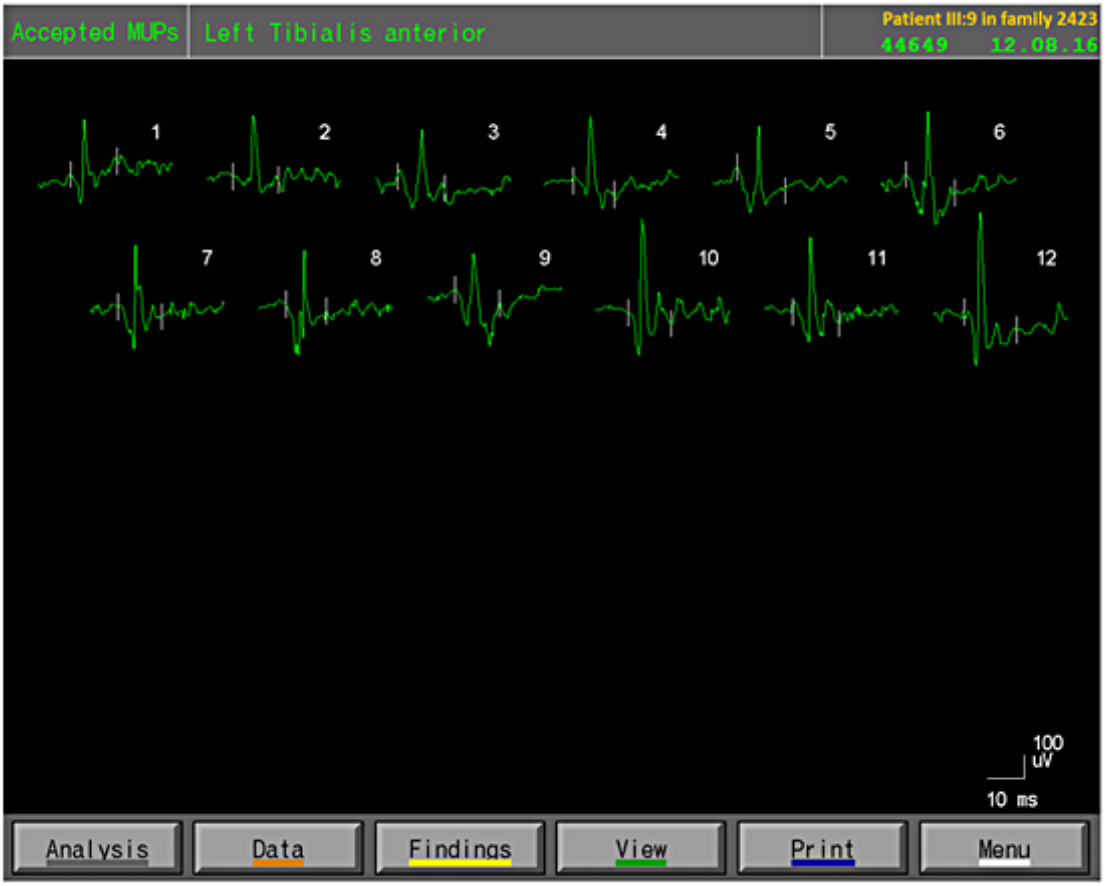

Figure S6 Structural comparison of wild-type and point mutants in the AIFM1 protein. (A and B) Location of the four mutant residues in the first FAD and the NADH domains of human AIFM1 (yellow arrows). Structure analysis of the wild-type AIFM1 (PDB ID: 4LII, generated by SWISS-MODEL program) indicates T260, L344 and G360 residues are located on the surface of mature protein and exposed to the solvent (white arrows). The mutated residue T260A in the first FAD domain and G360R in NADH domain (yellow circles) may have a greater impact on the protein functionality. (C and D) Location of the five identified amino acid substitutions (yellow arrows) in the second FAD domain. Their corresponding wild-type residues (white arrows) are all located on the surface of the protein. Among these mutated residues, R430C, R422W and P475L may have more functional effects (yellow circles). (reference: http://nar.oxfordjournals.org/content/early/2014/04/29/nar.gku340.abstract?keytype=ref&ijkey=FrXy4oQwsZzEAsw). All figures were generated using PyMOL (reference: http://www.pymol.org/citing).

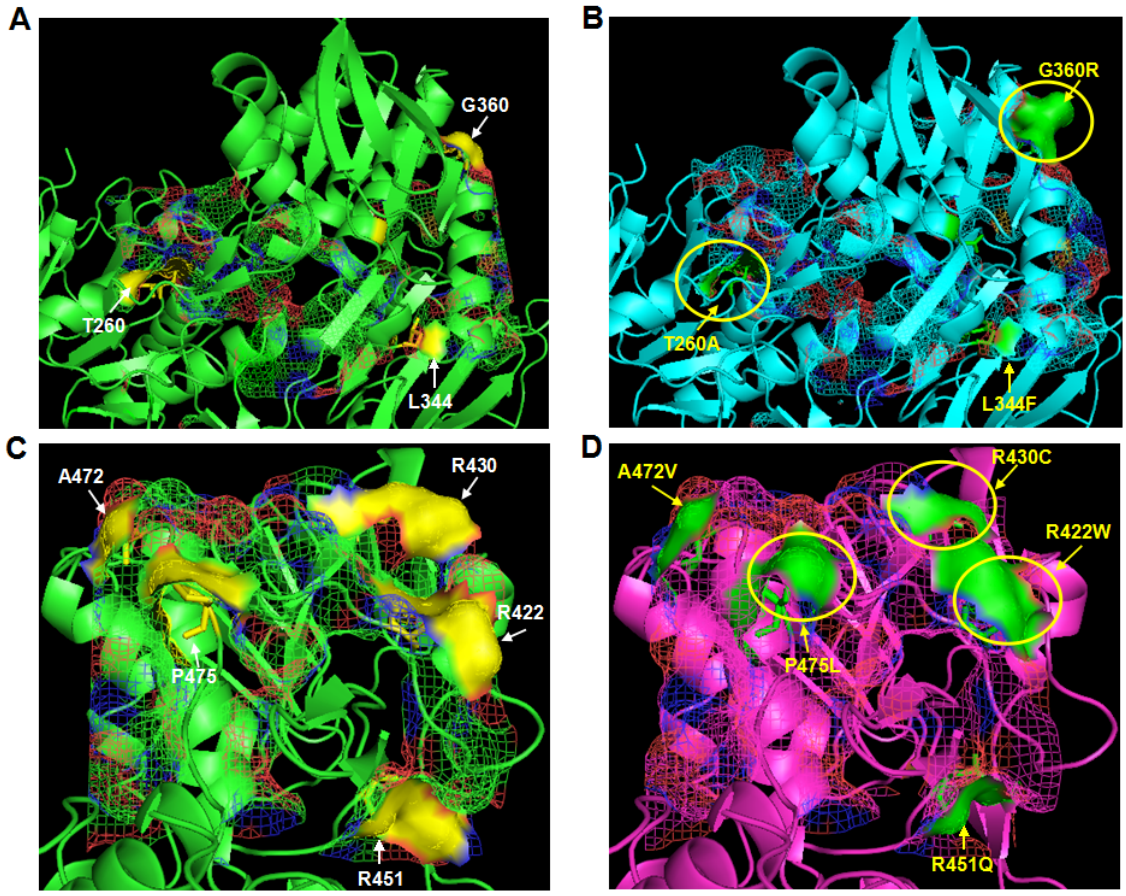

Figure S7 Locations of the two residues V498 and I591 (left panel) in C-terminus of AIFM1. Their mutated residues (right panel) have little effects on protein surface.

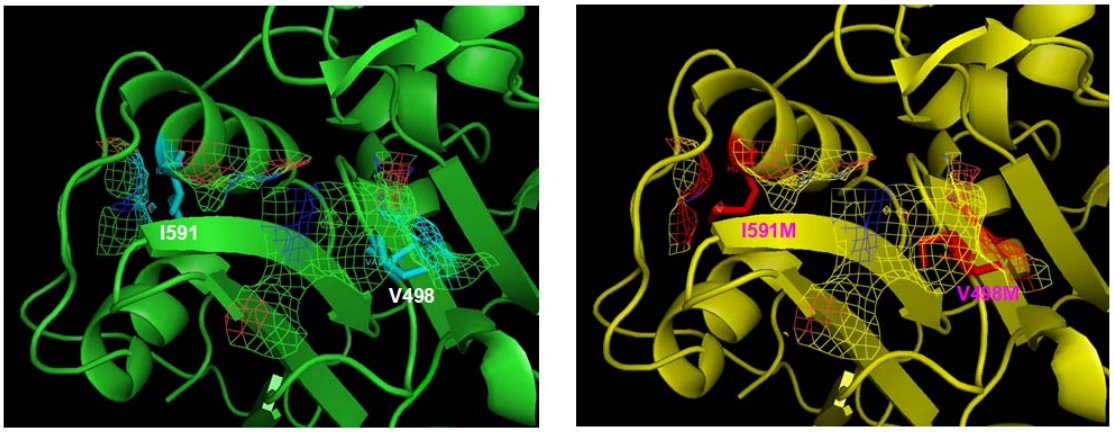

Figure S8 Localization of AIFM1 in stria vascularis. (A) Stria vascularis whole-mount preparation demonstrates the broad distribution of AIFM1. (B) The negative control without primary AIFM1 antibody. The scale bar indicates 15 μm.

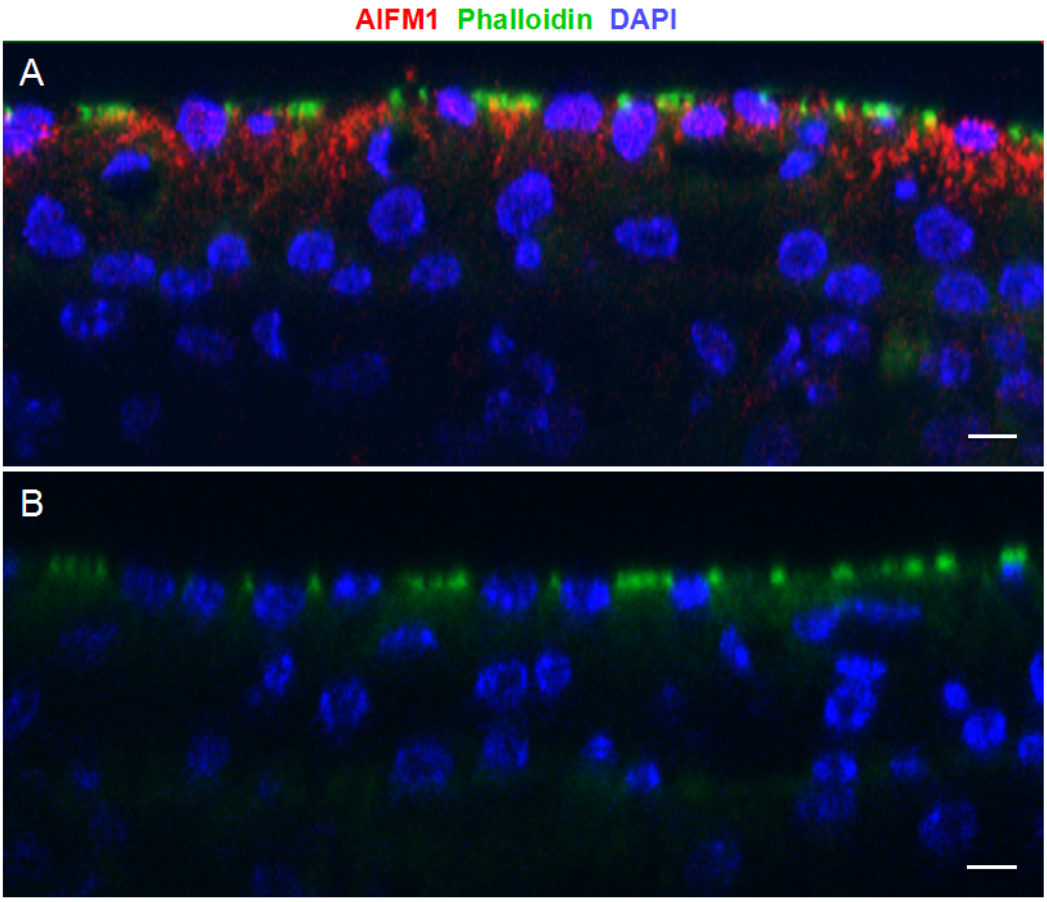

Figure S9 Localization of AIFM1 in vestibular tissue of murine inner ear. (A) Mouse macula of saccule labeled with AIFM1 antibody and phalloidin reveals AIFM1 localization to the hair cells. (B) The negative control without primary AIFM1 antibody. The scale bar indicates 15 μm.

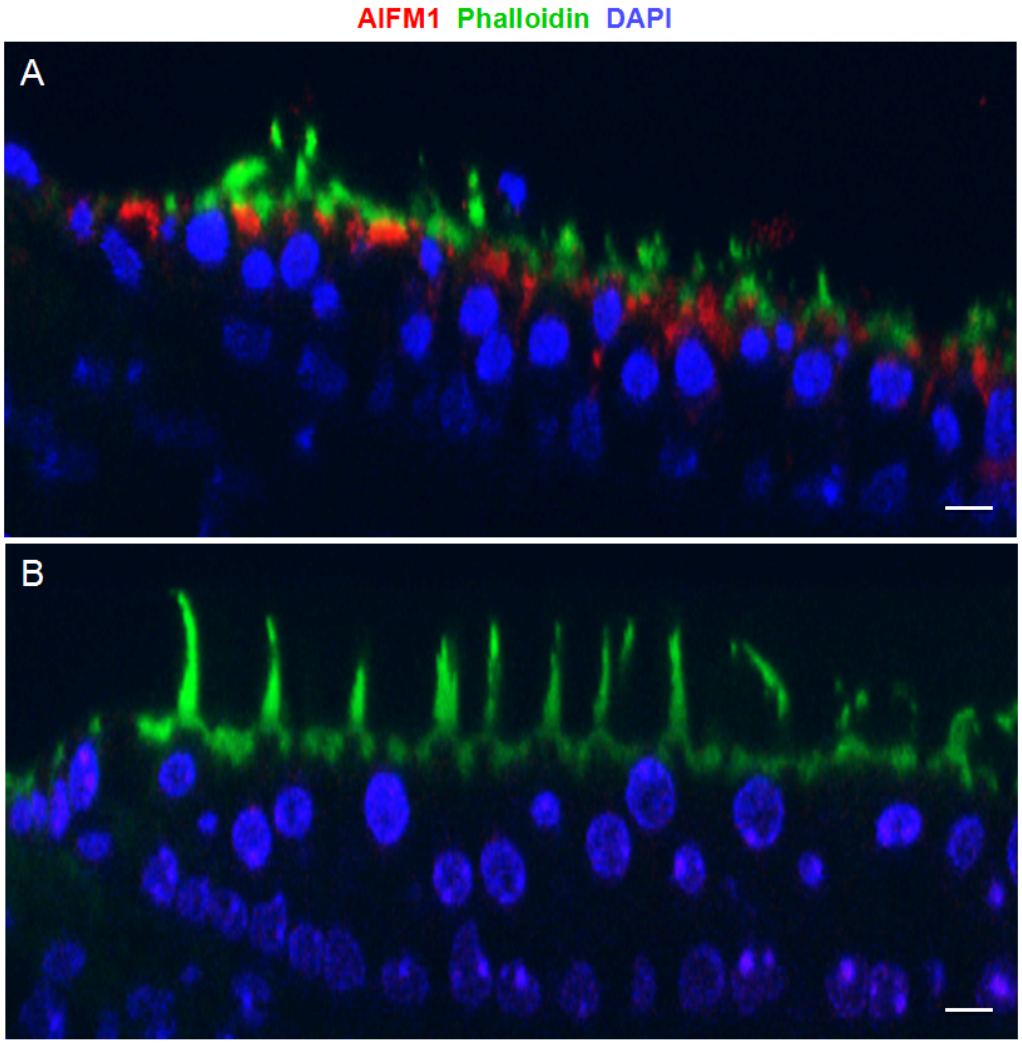

Figure S10 Age-of-onset distributions of auditory neuropathy (with or without peripheral neuropathy) patients with *AIFM1* mutations.

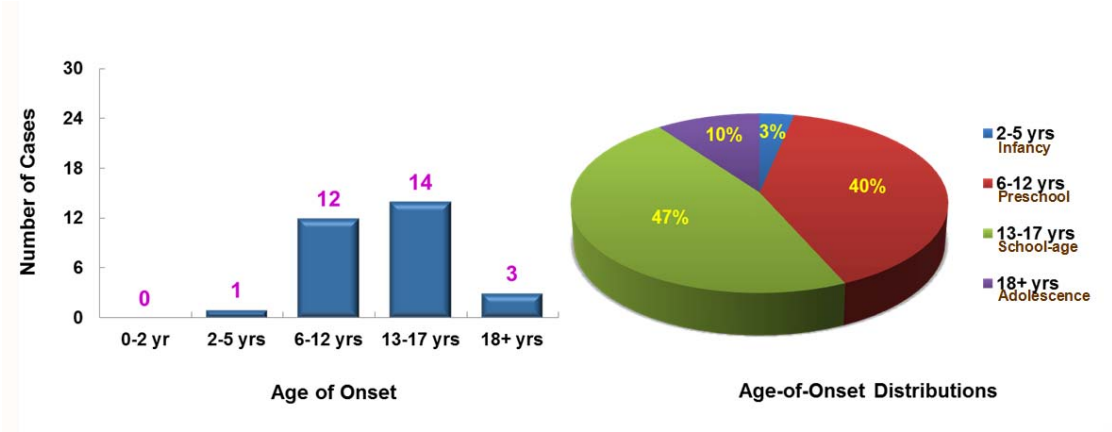

Supplementary Tables (S1-S13):

Table S1 PCR primer pairs information for candidate genes screening

Candidate genes	Screened region	Forward Primer (5'-3')	Reverse Primer (5'-3')	PCR Products Size (bp)
AIFM1	Exon1	GCTACGCTGTTGTGAGATGCT	GCCGACTACTGGGTTCAAATC	788
AIFM1	Exon2	ATCTGTGGGCAATAAGTCT	AACATAGTGGCTTTCAAGT	506
AIFM1	Exon3	GAGCCTAAAAATCTGAAACT	ATAACTTTCCCTTTGTGAG	393
AIFM1	Exon4 & 5	GTGGCAAAGAATCATCTGAG	CTTGCCCTTTGTAGACTGTT	616
AIFM1	Exon6	CCCCAAGTTGAGAACCACT	GGAAACACACATCACCATACT	358
AIFM1	Exon7	TTGGGGTGGTGATGGAAAT	GAAGGCTGGACTCTAAAACT	337
AIFM1	Exon8	ACCCCTTGAAGACAGACTC	TGGGGACTGCAAGATTATAC	362
AIFM1	Exon9	TGCCCTGACAACCAAAAAT	ATCCTGCCAAACACATCTCT	465
AIFM1	Exon10	CCTGCTGCTCCTTTACTTCT	ACTGGAGAATGGTGGAAACA	325
AIFM1	Exon11	TTCCACCATTCTCCAGTCAG	GCAAGGGGAGTGGAGAAC	374
AIFM1	Exon12	GTGGTGGAGGCTTATGAAAT	CTCAGCCTCCAAACACTCT	431
AIFM1	Exon13	TGAGCCCCCAAAGTTTAT	ATCTCCATTCATTCACCTAGT	507
AIFM1	Exon14	TGTGCTACCGTGTCATTCCT	TGCCAAATCTCAGACCACT	361
AIFM1	Exon15	GGAGGGAAGTTTAGGGTCAG	GGCACCCGATGAAGTTACAG	521
AIFM1	Exon16	CGGCTTAGAAACATTCCTG	AGGAGTTTTGCGTCTGGAGT	707
HS6ST2	Exon6	CAAAAGCGTATTGAGGGACTG	CAGGTTCTGATTGGCATTCG	246

Table S2 Summary of WES data for each sample of family 0223

Exome Capture Statistics	II: 1 (control)	III: 1 (affected)	III: 3 (affected)
Initial bases on target	50390601	50390601	50390601
Initial bases on or near target	124292823	124292823	124292823
Total effective reads	137440891	115293941	119954353
Total effective yield(Mb)	12145.66	10197.76	10602.99
Number of reads uniquely mapped to genome	131369753	110497810	114693978
Number of reads uniquely mapped to target	94420833	80077072	81339103
Effective sequences on target(Mb)	7258.88	6150.15	6240.29
Average sequencing depth on target	**144.05**	**122.05**	**123.84**
Coverage of target region	**99.90%**	**99.80%**	**99.80%**
Average read length(bp)	88.37	88.45	88.39
Mismatch rate in target region	0.30%	0.29%	0.30%
Fraction of effective bases on target	59.80%	60.30%	58.90%
Fraction of effective bases on or near target	80.10%	80.60%	79.50%
Fraction of uniquely mapped on target	71.90%	72.50%	70.90%
Fraction of target covered >=20x	97.10%	96.40%	96.40%
Fraction of target covered >=10x	98.90%	98.60%	98.60%
Fraction of target covered >=4x	99.60%	99.50%	99.50%
Coverage of flanking region	98.40%	98.00%	98.30%

Fraction of flanking region covered >=20x	50.50%	44.80%	47.50%
Fraction of flanking region covered >=10x	71.30%	66.20%	69.30%
Fraction of flanking region covered >=4x	90.10%	87.50%	89.30%
Mapping rate	99.41%	99.50%	99.41%
Duplicate rate	8.85%	8.20%	8.42%
Gender test result	Male	Male	Male

Table S3 Summary of SNPs and Indels for each sample of family 0223

Items/Samples	0400223-1	0400223-2	400223
Total SNPs	**90642**	**86156**	**89213**
Novel	876	786	832
Hom	41693	40068	41008
Het	48949	46088	48205
Synonymous	10122	9973	10080
Missense	9006	8818	8985
Stopgain	56	63	63
Stoploss	28	32	30
Startgain	270	236	268
Startloss	19	18	21
Exonic	20832	20485	20790
Splicing	79	68	74
Total Indels	**12091**	**11278**	**11481**
Novel	732	587	617
Hom	5666	5428	5533
Het	6425	5850	5948
Frameshift	226	208	209
Non-frameshift Insertion	82	86	85

Non-frameshift Deletion	92	89	83
Non-frameshift codon substitution	0	0	0
Non-frameshift codon substitution plus Insertion	21	17	20
Non-frameshift codon substitution plus Deletion	53	63	50
Stopgain	2	2	2
Stoploss	7	8	8
Startgain	0	0	0
Startloss	4	5	5
Exonic	751	735	731
Splicing	55	55	56

Note: The value of the first column takes the following precedence: exonic = splicing >ncRNA>> UTR5/UTR3 > intron > upstream/downstream >intergenic.

(1) Hom: homozygous; Het: heterozygous.

(2) Exonic here refers only to coding exonic portion, but not UTR portion.

(3) For SNPs, stopgain means that a nonsynonymous SNV that lead to the immediate creation of stop codon at the variant site. Meanwhile stoploss means that lead to the immediate elimination of stop codon at the variant site.

(4) Splicing is defined as variant that is within 2-bp away from an exon/intron boundary.

(5) Frameshift mutation means that an insertion/deletion of one or more nucleotides that cause frameshift changes in protein coding sequence.

(6) Nonframeshift mutation means that an insertion/deletion of 3 or multiples of 3 nucleotides that do not cause frameshift changes in protein coding sequence.

(7) Non-frameshift codon substitution means that one or many codons are changed, an MNP of size multiple of 3; Non-frameshift codon substitution plus Insertion (Deletion) means that One codon is changed and one or many codons are inserted (deleted). An insert (deletion) of size multiple of three, not at codon boundary.
(8) For Indels, stopgain means that a frameshift insertion/deletion, nonframeshift insertion/deletion or block substitution that lead to the immediate creation of stop codon at the variant site. For frameshift mutations, the creation of stop codon downstream of the variant will not be counted as "stopgain".Meanwhile stoploss means that lead to the immediate elimination of stop codon at the variant site.

Table S4 Screening and identifying the causal genes by WES (SNPs[#])

Feature SNP	II: 1 (control)	III: 1 (affected)	III: 3 (affected)
Total SNPs	90642	86156	89213
Filtered_dbSNP	74850	71038	73573
Filtered_dbSNP_1000G	3346	3138	3237
Filtered_dbSNP_1000G_Hapmap	3113	2921	3012
Filtered_dbSNP_1000G_Hapmap_YH	2744	2549	2640
Filtered_dbSNP_1000G_Hapmap_YH_Ctr1	0	1220	1318
Share all cases		561	

[#]Function: missense|readthrough|nonsense|spliceSite|synonymous-coding|5-UTR|3-UTR|intron|intergenic

Table S5 Screening and identifying the causal genes by WES (Indels[#])

Feature indels	II: 1 (control)	III: 1 (affected)	III: 3 (affected)
Total Indels	3379	3266	3273
Filtered_dbIndel	2275	2193	2217
Filtered_dbIndel_1000G	2043	1961	1985
Filtered_dbIndel_1000G_Hapmap	2043	1961	1985
Filtered_dbIndel_1000G_Hapmap_YH	2042	1960	1984
Filtered_dbIndel_1000G_Hapmap_YH_Ctrl	0	462	455
Share all cases		245	

[#]Function: frameshift|cds-indel|spliceSite|5-UTR|3-UTR|intron|promoter|intergenic

Table S6 Screening and identifying the causal genes by WES (Functional SNPs[#])

Feature SNP	II: 1 (control)	III: 1 (affected)	III: 3 (affected)
Functional_SNPs	12540	12344	12541
Filtered_dbSNP	10349	10172	10371
Filtered_dbSNP_1000G	599	609	614
Filtered_dbSNP_1000G_Hapmap	575	586	590
Filtered_dbSNP_1000G_Hapmap_YH	525	532	537
Filtered_dbSNP_1000G_Hapmap_YH_Ctr1	0	260	285
Share all cases		129	

[#]Function: missense|readthrough|nonsense|spliceSite

Table S7 Screening and identifying the causal genes by WES (Functional Indels[#])

Feature indels	II: 1 (control)	III: 1 (affected)	III: 3 (affected)
Functional Indels	1170	1141	1148
Filtered_dbIndel	769	754	769
Filtered_dbIndel_1000G	706	688	696
Filtered_dbIndel_1000G_Hapmap	706	688	696
Filtered_dbIndel_1000G_Hapmap_YH	705	687	695
Filtered_dbIndel_1000G_Hapmap_YH_Ctrl	0	169	158
Share all cases		84	

[#]Function: frameshift|cds-indel|spliceSite

Table S8 Candidate variants shared by two affected individuals of family 0223

Chromosome	Position	Reference	Change	Gene	Codon	Substitution
ChrX	129271098	C	T	AIFM1	Ctc1030Ttc	L344F
Chr4	120550141	-3GCA	/	PDE5A	5-UTR	Deletion
Chr3	73651621	-1A	/	PDZRN3	Splice site	Deletion
Chr12	42853058	-1T	/	PRICKLE1	3-UTR	Deletion
Chr2	202344179	-1T	/	STRADB	NR_exon	Deletion

/, not presenting the base substitution; NR_exon, non-coding exon variant.

Table S9 Audiological test data of cases with *AIFM1* mutations

Case ID	Age of onset (yrs)	Age at test (yrs)	Hearing level		SDS (%)		Tymp		Stapedial reflex		ABR[c]		DPOAE[d] (kHz)		ECochG[e]	
			PTA[b]	Audiogram	L	R	L	R	L	R	L	R	L	R	L	R
7170[a]	19	20	28.75	up-slope	48	84	A	As	/	/	NR	NR	0.75-4, 8	0.75-4, 8	1.02	0.64
0223[a]	16	27	35.00	up-slope	12	20	A	A	/	/	NR	NR	0.5-8	0.5-8	NR of AP	1.47
1302	17	20	36.25	up-slope	60	52	A	A	/	/	NR	NR	0.75-8	0.75-8	NA	NA
1757	19	19	32.5	up-slope	84	92	A	A	/	/	Vt=6.35ms,miss--ing waves I-III		0.5-8	0.75-8	NA	NA
7187	13	25	41.25	up-slope	NA	NA	A	A	/	/	NR	NR	0.75-8	0.75-6	0.56	0.77
1747	14	17	46.25	up-slope	0	20	A	A	/	/	NR	NR	0.5-8	0.5-3, 6	0.96	1.72
2724[a]	18	31	48.75	up-slope	36	12	A	A	/	/	NR	NR	0.5-8	0.5-8	1.12	1.76
3033	13	16	38.75	inverted U-shape	64	52	A	A	/	/	NR	NR	0.75-8	1-3, 8	0.83	NR of AP
6962	15	20	36.25	up-slope	60	52	A	A	/	/	NR	NR	0.75-8	0.75-8	NA	NA
2423[a]	14	36	47.50	up-slope	16	20	A	A	/	/	NR	NR	0.5-8	0.5-3, 6, 8	0.83	1.00
0077	7	15	32.50	U-shape	NA	NA	A	A	/	/	NR	NR	0.5-8	0.5-8	NA	NA
AUNX1[a]	16	27	43.75	flat	0	0	A	A	/	/	NR	NR	0.5-3, 8	0.5-8	>1	0.71
1806	8	20	40.00	up-slope	16	44	A	A	/	/	NR	NR	0.5, 1-8	0.5-8	0.55	0.68
0046	14	24	56.25	up-slope	NA	NA	A	A	/	/	NR	NR	0.5, 1.5-8	0.5-8	>1	>1
4678	5	14	51.25	up-slope	NA	NA	A	A	/	/	NR	NR	0.75-8	0.75-8	NA	NA

3305	11	15	32.50	U-shape	48	56	A	A	/	/	NR	NR	0.75-8	0.75-8	1.22	2.60	

[a] the familial case, representing the proband of the AN family.

[b] PTA, pure-tone air-conduction averages (0.5, 1, 2 and 4 kHz) for the better-hearing ear of the affected subjects (dB HL).

[c]. ABR was evoked by the click stimulus at maximum intensity level (100 dB nHL).

[d] the frequencies with DPOAE response in normal level.

[e] Click-evoked ECochG was recorded at the stimulating intensity of 100 dB nHL, and analyzed by the amplitude ratio of –SP/AP.

AN, auditory neuropathy; SDS, the speech discrimination score; Tymp, tympanometry; /, absent of stapedial reflex; ABR, auditory brainstem response; nHL, normal hearing level; DPOAE, distortion product otoacoustic emission; ECochG, electrocochleogram; SP/AP, summating potential/action potential; NA, not available; NR, no response; Vt, wave V potential time.

Table S10 The allele frequency of total eleven identified *AIFM1* variants from genetic variation databases

Variants	1000G_ALL	1000G_EAS	1000G_AFR	1000G_AMR	1000G_EUR	ESP 6500_ALL	ESP 6500_AA	ESP 6500_EA	dbSNP (142)	Controls*
c.778A>G (p.T260A)	—	—	—	—	—	—	—	—	—	—
c.1030C>T (p.L344F)	0.000529801	0.002	—	—	—	—	—	—	NA (rs184474885)	—
c.1078G>C (p.G360R)	—	—	—	—	—	—	—	—	—	—
c.1264C>T (p.R422W)	—	—	—	—	—	—	—	—	—	—
c.1265G>A (p.R422Q)	—	—	—	—	—	—	—	—	—	—
c.1288C>T (p.R430C)	—	—	—	—	—	—	—	—	—	—
c.1352G>A (p.R451Q)	—	—	—	—	—	—	—	—	—	—
c.1415C>T (p.A472V)	—	—	—	—	—	—	—	—	—	—
c.1424C>T (p.P475L)	—	—	—	—	—	—	—	—	—	—
c.1492G>A (p.V498M)	—	—	—	—	—	—	—	—	—	—
c.1773C>G (p.I591M)	—	—	—	—	—	—	—	—	—	—

* Controls in this study included 500 healthy ethnicity-matched individulas (125 males and 125 females with normal hearing, 750 X chromosomes).

1000G_ALL, allele frequency in all populations in the 1000 Genomes project; 1000G_EAS, allele frequency in East Asian populations in the 1000 Genomes project; 1000G_AFR, allele frequency in African populations in the 1000 Genomes project; 1000G_AMR, allele frequency in American populations in the 1000 Genomes project; 1000G_EUR, allele frequency in European populations in the 1000 Genomes project; ESP 6500_ALL, allele frequency in all subjects in the NHLBI ESP 6500 exomes; ESP 6500_AA, allele frequency in African Americans in the NHLBI ESP 6500 exomes; ESP 6500_EA, allele frequency in European Americans in the NHLBI ESP 6500 exomes; dbSNP (142), the database of Short Genetic Variations (human Build 142); —, negative finding; NA, the allele frequency is not available.

Table S11 Nerve conduction velocities in seven familial ANSD cases accompanied by late-onset peripheral neuropathy

Family	Patient	Course of AN/PN (yrs)	Side (L/R)	Tibial motor		Peroneal motor		Median motor		Ulnar motor		Sural sensory		Median sensory		Ulnar sensory	
				CV	Amp	CV	Amp	CV	Amp	CV	Amp	CV	Amp	CV	Amp	CV	Amp
AUNX1	III:22	11/1	L	44.2	*8.5*	45.8	*4.4*	56.4	*17.2*	57.8	*7.6*	NR	NR	47.1	3.7	44.8	3.1
					9.3		**5.8**		**17.5**		**7.5**						
			R	44.7	9.9	45.8	*4.4*	57.9	*7.5*	55.3	*7.0*	NR	NR	NR	NR	38.2	0.7
					10.7		**4.3**		**8.1**		**7.4**						
	III:23	19/0.5	L	43.5	*6.9*	43.8	*3.6*	58.3	*13.1*	56.5	*7.6*	NR	NR	NR	NR	NR	NR
					7.6		**3.9**		**13.6**		**7.8**						
			R	44.6	*4.7*	43.1	*4.3*	NT	*NT*	NT	*NT*	NR	NR	NR	NR	NR	NR
					4.6		**4.5**		**NT**		**NT**						
7170	IV:2	19/2	L	48.8	*21.4*	48.5	*4.5*	59.0	*18.2*	55.6	*18.3*	NR	NR	NR	NR	NR	NR
					25.0		**3.2**		**18.7**		**18.6**						
			R	52.5	*20.1*	50.8	*5.5*	NT	*NT*	NT	*NT*	40.5	2.3	42.1	0.8	NR	NR
					23.5		**6.4**		**NT**		**NT**						
2724	III:4	19/10	L	51.3	*10.1*	53.6	*6.6*	61.1	*21.0*	57.8	*12.2*	NR	NR	57.7	0.9	NR	NR
					10.1		**6.9**		**21.4**		**12.6**						
			R	52.0	*8.0*	50.0	*8.3*	NT	*NT*	NT	*NT*	NR	NR	60.0	1.0	NR	NR
					11.7		**6.0**		**NT**		**NT**						
2423	III:1	29/27	L	48.2	*15.1*	45.2	*12.4*	53.7	*13.6*	54.9	*15.0*	37.5	3.3	47.1	3.3	32.6	2.6
					17.4		**13.5**		**14.7**		**17.4**						
			R	47.1	*18.8*	45.2	*9.5*	55.0	*16.1*	56.0	*15.8*	42.9	2.0	51.6	3.0	41.2	2.4

				20.5		**10.0**		**16.4**		**16.0**						
III:9	22/4	L	43.3	*9.2*	46.3	*18.2*	56.4	*20.7*	60.0	*12.8*	NR	NR	32.7	1.2	32.4	0.9
				10.6		**18.1**		**22.2**		**12.9**						
		R	44.3	*7.5*	46.3	*18.2*	56.4	*19.3*	55.1	*14.7*	NR	NR	NR	NR	34.3	1.5
				9.9		**14.2**		**21.3**		**15.5**						
	28/10	L	47.0	*7.8*	47.7	*11.6*	66.7	*20.6*	56.2	*10.7*	NR	NR	44.4	1.5	37.5	0.4
				10.3		**10.8**		**21.2**		**10.8**						
		R	44.8	*8.2*	49.2	*11.8*	NT	*NT*	NT	*NT*	NR	NR	NT	NT	NT	NT
				9.5		**9.3**		**NT**		**NT**						
III:11	18/5	L	48.7	*16.2*	48.4	*28.7*	56.4	*18.3*	55.1	*17.1*	NR	NR	51.6	3.5	52.0	2.1
				18.7		**30.4**		**19.2**		**17.4**						
		R	45.8	*20.7*	48.4	*19.6*	55.0	*16.7*	52.9	*21.1*	40.5	1.1	50.0	2.1	46.4	3.6
				22.0		**24.1**		**16.7**		**23.2**						

The italic represents proximal stimulation, and the boldface represents distal stimulation. PN, late-onset peripheral neuropathy; L/R, left/right; CV, conductin velocity (m/s); Amp, amplitude (mV for motor; μV for sensory); NR, no response; NT, not tested. The abnormal values are shown in red. Normal CVs: motor tibial ≥ 40.0, peroneal ≥ 40.0, median ≥ 50.0, and ulnar ≥ 50.0; sensory sural ≥ 50.0, median ≥ 50.0, and ulnar ≥ 50.0. Normal amplitudes: motor tibial ≥ 5.0, peroneal ≥ 3.0, median ≥ 5.0, and ulnar ≥ 5.0; sensory sural ≥ 2.0, median ≥ 2.0, and ulnar ≥ 2.0.

Table S12 Missense mutations pathogenicity prediction of *AIFM1* using in silico bioinformatic tools

Mutations	Associated case ID	Polyphen2 prediction				SIFT prediction		PROVEAN prediction		Mutation assessor		Related protein domain
		Result	Score	Sensitivity	Specitivity	Result	Score	Result[a]	Score	Func. impact[b]	Score	
p.T260A	Family 7170	Possibly damaging	0.858	0.830	0.930	Damaging	0.010	Deleterious	-4.631	High	4.010	FAD-binding
p.L344F	1302, 1757, 7187 and family 0223	Possibly damaging	0.846	0.83	0.930	Tolerated	0.150	Deleterious	-3.554	Medium	2.150	NADH-binding
p.G360R	1747	Probably damaging	1.000	0.000	1.000	Damaging	0.000	Deleterious	-7.948	High	3.955	NADH-binding
p.R422W	3033, 6962 and family 2724	Probably damaging	1.000	0.000	1.000	Tolerated	0.090	Deleterious	-4.281	Medium	2.740	FAD-binding
p.R422Q	Family 2423	Probably damaging	1.000	0.000	1.000	Tolerated	0.640	Neutral	-1.974	Medium	2.045	FAD-binding
p.R430C	0077	Probably damaging	1.000	0.000	1.000	Damaging	0.010	Deleterious	-7.948	Medium	2.390	FAD-binding
p.R451Q	Family AUNX1	Probably damaging	1.000	0.000	1.000	Damaging	0.000	Deleterious	-3.970	High	3.520	FAD-binding
p.A472V	1806	Benign	0.170	0.920	0.870	Damaging	0.030	Deleterious	-3.373	Medium	2.750	FAD-binding
p.P475L	0046	Possibly damaging	0.517	0.880	0.900	Damaging	0.020	Deleterious	-8.993	Medium	2.690	FAD-binding
p.V498M	4768	Probably damaging	1.000	0.000	1.000	Damaging	0.020	Deleterious	-2.664	Medium	2.300	C-terminal
p.I591M	3305	Possibly damaging	0.898	0.820	0.940	Tolerated	0.110	Neutral	-2.093	Low	1.910	C-terminal

[a] For the PROVEAN prediction result, the cutoff score was -2.500.

[b] Func. impact, functional impact of a variant: predicted functional (high, medium) and predicted non-functional (low, neutral).

Table S13 Different phenotypes of diseases caused by *AIFM1* mutations

Family origin	Phenotype	Age of onset	Diagnosis	Mutation	Reference
China	auditory neuropathy accompanied with delayed peripheral sensory neuropathy, and hypoplasia of bilateral cochlea nerves showed by MRI	School age & adolescence (average of 12.6 yrs)	AUNX1/DFNX5	11 mutations (pls see table 1)	this study
America	Motor-sensory axonal neuropathy, bilateral sensorineural hearing loss, mental retardation, and abnormal MRI signals in the white matter	childhood (from birth)	Cowchock syndrome	c.1478A>T (p.E493V)	Rinaldi C et al. (2012)
Palestinian	choroids plexus cysts, bilateral brain ventriculomegaly, enlarged cisterna magna, swallowing difficulties, hypotonic with muscle weakness and atrophy	prenatal	Prenatal ventriculomegaly	c.923G>A (p.G308E)	Berger I et al. (2011)
Italy	psychomotor regression, muscle weakness and atrophy, lack of further development, and abnormal MRI signals in the basal ganglia	~1 year of age	COXPD6	c.601–603del (p.R201del)	Ghezzi D et al. (2010)